

## Design and synthesis of Kekulé and non-Kekulé diradicaloids via radical peri-annulation strategy: the power of seven Clar's sextets

Febin Kuriakose,<sup>†</sup> Ökten Üngör,<sup>†</sup> Debashis Sen,<sup>†</sup> Frederic Mentink-Vigier,<sup>‡</sup> Xinsong Lin,<sup>†</sup>  
Shubham Bisht,<sup>†</sup> Robert A. Lazenby,<sup>†</sup> Michael Shatruk,<sup>†</sup> Igor V. Alabugin<sup>†\*</sup>

<sup>†</sup>: Department of Chemistry and Biochemistry, Florida State University, Tallahassee, FL -  
32306-4390 (USA) E-mail: alabugin@chem.fsu.edu

<sup>‡</sup>: National High Magnetic Field Laboratory, Tallahassee, FL, USA

### ABSTRACT

This work introduces an approach to uncoupling electrons via maximum utilization of localized aromatic units, i.e., the Clar's  $\pi$ -sextets. To illustrate the utility of this concept to the design of Kekulé diradicaloids, we have synthesized a tridecacyclic polyaromatic system where a gain of five Clar's sextets in the open shell form overcomes electron pairing and leads to the emergence of high degree of diradical character. According to unrestricted symmetry-broken UCAM-B3LYP DFT calculations, the singlet diradical character in this core system is characterized by the  $y_0$  value of 0.98 ( $y_0 = 0$  for closed shell molecule,  $y_0 = 1$  for pure diradical). The efficiency of the new design strategy was evaluated by comparing the Kekulé system with an isomeric non-Kekulé diradical of identical size, i.e., a system where the radical centers cannot couple via resonance and the high-spin ground state is unavoidable. The calculated singlet-triplet gap, i.e., the  $\Delta E_{ST}$  values, in both of these systems approach zero: -0.3 kcal/mol for the Kekulé and +0.2 kcal/mol for the non-Kekulé diradicaloids.

The target isomeric Kekulé and non-Kekulé systems were assembled using a sequence of radical *peri*-annulations, cross-coupling and C-H activation. The diradicals are kinetically stabilized by six *tert*-butyl substituents and (triisopropylsilyl)acetylene groups. The Kekulé diradicaloid (**K**) has a half-life of 42 h under ambient conditions (i.e., exposure to air at the room temperature) while the non-Kekulé diradicaloid (**NK**) has a half-life of 2h. Both molecules are NMR-inactive but EPR-active at room temperature. The magnetic properties of the Kekulé diradicaloid was studied by superconducting quantum interference device (SQUID) to provide the experimental singlet-triplet energy gap,  $\Delta E_{ST}$  (**K**) = -0.8 kcal/mol, which was close to calculated value. Cyclic voltammetry revealed quasi-reversible two-electron oxidation and reduction processes, consistent with the presence of two degenerate partially occupied molecular orbitals.

## INTRODUCTION

Due to the presence of singly occupied nonbonding molecular orbitals (MOs), open shell polycyclic aromatic hydrocarbons (PAHs) display unique optical, electronic and magnetic properties.<sup>1-6</sup> PAHs that possess *two* unpaired electrons at two low-energy singly-occupied nonbonding MOs can be described as diradicaloids. The degree of coupling between these electrons determines relative contributions of the closed-shell form and the open-shell form to the overall electronic structure and defines the singlet-triplet gap,  $\Delta E_{ST}$ .<sup>7</sup> These electronic features can lead to enhanced polarizability and impressive third order nonlinear optical properties.<sup>8-12</sup> The electronic nature of open-shell diradicaloids also lends itself for the development of the singlet fission processes that can increase efficiency of the future photovoltaic devices.<sup>13-18</sup>

The two conceptually different approaches to conjugated diradicals are based on Kekulé vs. non-Kekulé structures. The non-Kekulé structures have open-shell character because of their intrinsic bonding pattern that prevents the radical centers from coupling via resonance. In contrast, the open-shell character in the Kekulé diradicals is only generated when the open-shell diradical resonance structure can overcome the “classic” closed-shell preference due to a combination of sufficiently strong electronic factors.

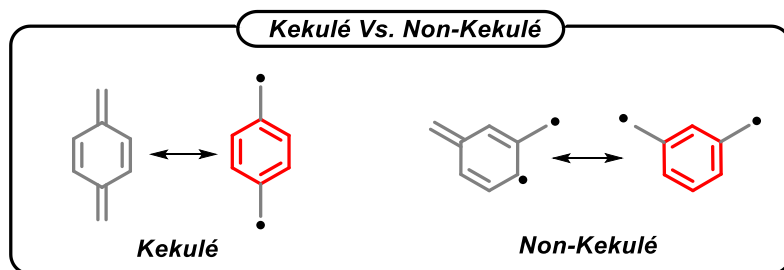


**Figure 1.** Kekulé vs. Non-Kekulé diradicals

The challenge for making Kekulé diradicals is that the two radical centers formally originate from uncoupling of two paired electrons, i.e., the effective loss of one chemical bond. For the same reasons why, the formation of chemical bonds is inherently favorable and can be considered as a cornerstone of molecular science, *losing* a chemical bond to form a diradical is inherently unfavorable. Although uncoupling electrons in a  $\pi$ -bond comes with a smaller penalty than breaking a  $\sigma$ -bond, the penalty is still significant as one can glimpse from the 81 kcal/mol energy difference between the ground state and the triplet state of ethylene (i.e, the singlet/triplet (S/T) gap<sup>19</sup>). This penalty for losing a bond can be decreased by additional factors that favor the diradical form, e.g., extended conjugation, gain of aromatic stabilization,<sup>20,21</sup> loss of antiaromaticity<sup>22-28</sup> etc.

In this work, we will concentrate on using localized aromaticity, i.e., the Clar's  $\pi$  sextets in order to uncouple electrons in a  $\pi$  bond. The Clar's rule is one of the key ideas of general importance in chemistry of PAHs. This rule states that the Kekulé resonance structure with the largest number of disjoint benzene-like aromatic  $\pi$ -sextets, i.e. "the Clar's sextets", contribute the most to the PAH properties. The larger number of Clar's sextets in one of the isomeric PAHs usually predicts its greater stability.<sup>29–33</sup>

Recent research has focused on Kekulé diradicaloids with a variety of edge structures such as peri-fused acenes,<sup>34–38</sup> bisphenalenyls,<sup>39–41</sup> zethrenes<sup>42–45</sup> and quinoidal rylene<sup>46–48</sup> (Figure 2). Although these structures are inherently unstable, chemical modifications with bulky groups and electron withdrawing groups can provide the varying degrees of kinetic protection. The degree of diradical character in singlet diradicaloids can be described by the diradical index  $y_0$ , which ranges from  $y_0=1$  (pure diradical) to  $y_0=0$  (pure closed shell).<sup>49,50</sup> Very recently, Chi and coworkers reported a kinetically stable [4,3] peri-acene diradicaloid with a large diradical character of  $y_0=0.94$ . The observed high diradical character can be attributed to the aromatic stabilization originating from the gain of five additional Clar's sextets in the open shell form.<sup>51,52</sup>

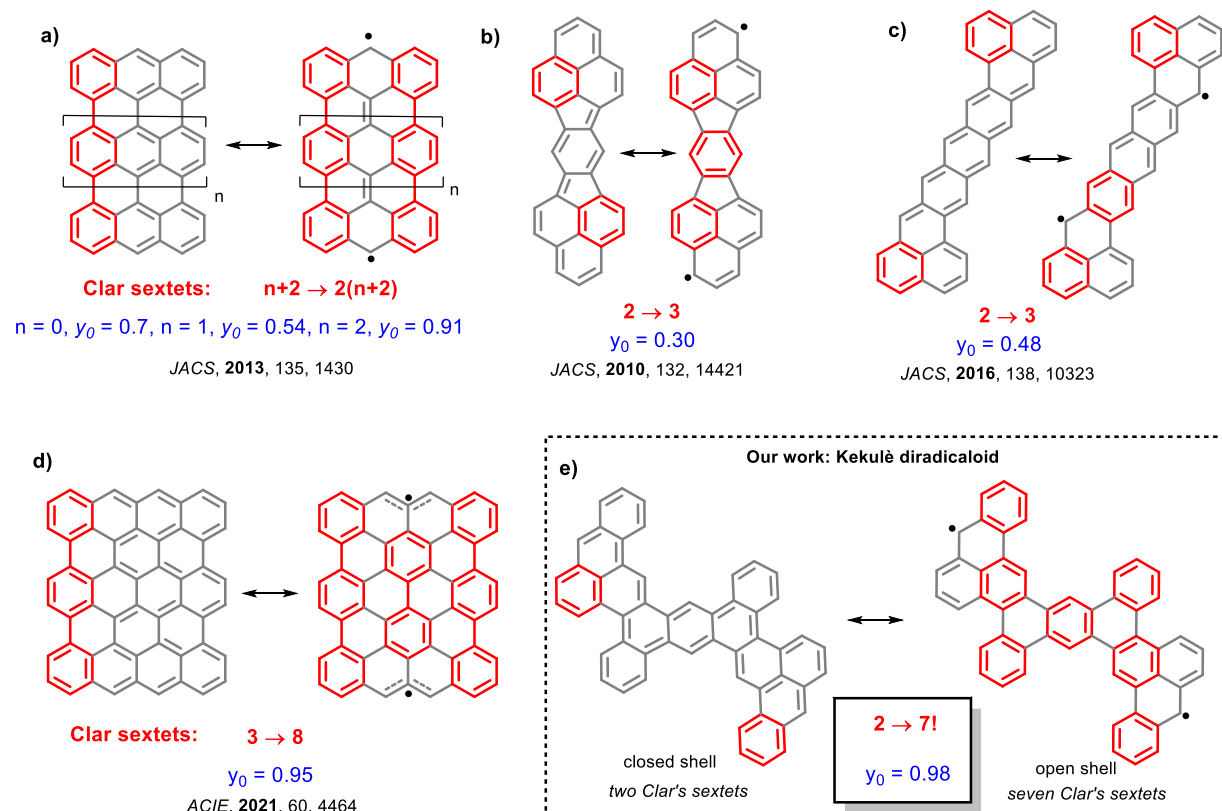


**Figure 2.** Literature designs of Kekulé diradicaloids: (a) peri-fused acenes, (b) bis-phenalenyl, (c) nonazethrene (d) [4,3]peri-acene with high diradical character (e) our design

Guided by the idea that high diradical character can be deduced qualitatively from Clar's rule and that gaining additional Clar's sextets in the open shell form is the key to obtaining a stable ground state singlet

diradicaloid with higher diradical character, we have considered a relatively simple, yet unknown, system shown in the bottom right corner of Figure 2e where the diradical formation is assisted by the occurrence of seven (!) Clar sextets. This polycyclic framework includes part of the “ideal” system for the design of diradicals that we will discuss below.

## RESULTS AND DISCUSSION

### The rational design of polyaromatic diradicals

The new design reported in this work originated from the question to what extent can one exploit the Clar's rule for the systematic search of molecules with high diradical character. The starting point is the idea that making the singlet diradicaloid electronically stable while having high degree of diradical character is facilitated by gaining the maximum number of Clar's aromatic sextets in the open shell form. Based on this idea, we propose a general approach to the design of novel diradicaloids in the following way. The starting point is simple - choose a system with the maximum number of Clar's sextets ( “fully benzenoid” in Clar's terms <sup>52</sup>) for a given ring system, add CH<sub>2</sub> radicals and explore the electron pairing topology. This is a systematic approach to interesting Kekulé and non-Kekulé diradicaloid topologies which have not explored previously. We give a full list of these diradicals in the SI and only give the illustrative examples and a summary below.

To start, let's add two para-CH<sub>2</sub> radicals to benzene. The resulting molecule has a quinoid ground state. Transforming it into a diradical would create only one Clar's sextet. Hence, the S/T gap is relatively large (~30 kcal/mol) and the  $y_0$  parameter of 0 indicates no diradical character. However, progressive expansion of the core to biphenyl, triphenylene, dibenzo[fg,op]tetracene, and tribenzo[f,k,m]tetraphene gradually changes the situation. Use of these cores allows one to progressively increase the number of Clar's sextets gained upon the conversion of quinoid structures to the diradical counterparts (two, three, four, and five additional Clar's sextets, respectively). Note the rapid decrease in the respective S/T gaps (5.1>1.9>0.8>0.4) and the concomitant increase in the  $y_0$  value (0.32<0.83<0.97<0.98). (Figure 3)

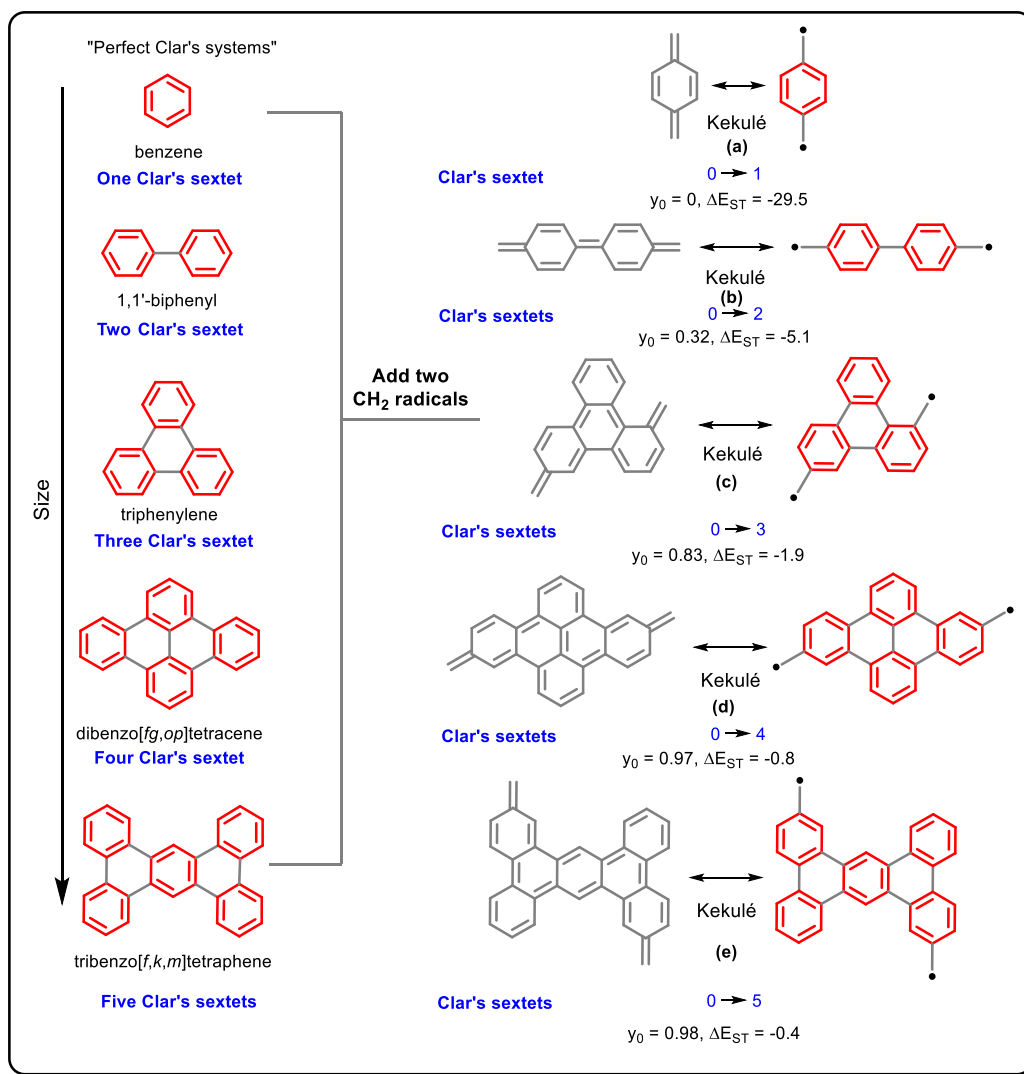


**Figure 3.** The introduction of diradical character into Kekulé polyaromatic systems based on the “ideal” systems with the maximum number of Clar’s sextets is facilitated in the larger systems. Calculations are performed at (U)CAM-B3LYP/6-31G(d,p) level of theory. See the SI for the full list of possibilities.

The number of possibilities is large because the  $\text{CH}_2$  “units” can be attached to the “ideal” polyaromatic cores in a variety of patterns. These patterns also include systems that are inherently incapable of electron pairing due to their topology. Such systems correspond to non-Kekulé structures. For example, adding two methylene radicals to triphenylene yielded a total of 16 unique results with ten Kekulé and six non-Kekulé structures (see the SI). For dibenzo[fg,op]tetracene, the appending of two methylene radicals yields the total of 27 diradicals, fifteen of which are Kekulé and twelve are non-Kekulé. The next step is tribenzo[f,k,m]tetraphene, PAH with the most number of Clar’s sextets for a seven ring system. Here, the process creates 45 different molecular systems – 25 Kekulé and 20 non-Kekulé (the full list of possibilities

is provided in the SI). This discussion illustrates the large amount of potential diradicals available when starting with the privileged polyaromatic cores with the maximum number of Clar's sextets.

However, not all of these systems are equal, as some of them do not lose all of their Clar's sextets upon electron pairing. Their contribution of diradical character depends greatly on the relative placement of the two spin centers. Based on the location of spin centers, these molecules can gain of one, two, three, four or five Clar's sextets in the open-shell. In fact, only a few of the 45 possibilities for the tribenzo[f,k,m]tetraphene show the maximum gain in the local Clar's aromaticity (see SI section for the full list). Computational analysis on the effect of the number of gained Clar's sextets on diradical character and singlet – triplet gap (Figure 4) found, as expected, that the structures with the greatest gain have the most diradical character. Overall, S/T gap decreases exponentially with the increase in the number of gained Clar's sextets in the open-shell form.

Figure 4 illustrates it quite clearly. Only one Clar's sextet is gained in compound **f** which has a closed-shell ground state with zero diradical character and a high singlet-triplet gap of -51 kcal/mol. Gain of two Clar's sextets in the isomer **g** introduces non-zero diradical character of  $y_0 = 0.32$  and the much lower S/T gap of -6.5 kcal/mol. As the gain in Clar's sextets increases, the degree of diradical character  $y_0$  increases ( $0 < 0.32 < 0.75 < 0.94 < 0.98$ ) and singlet triplet gap decreases ( $50.8 > 6.5 > 1.6 > 0.5 > 0.4$ ). The open-shell form of the bottom structure **e** gains maximum (five) Clar's sextets. As expected, this results in very high diradical character,  $y_0 = 0.98$  and very small singlet-triplet gap,  $\Delta E_{ST} = -0.4$  kcal/mol. (Figure 4). This is the system that was chosen for the experimental pursuit.

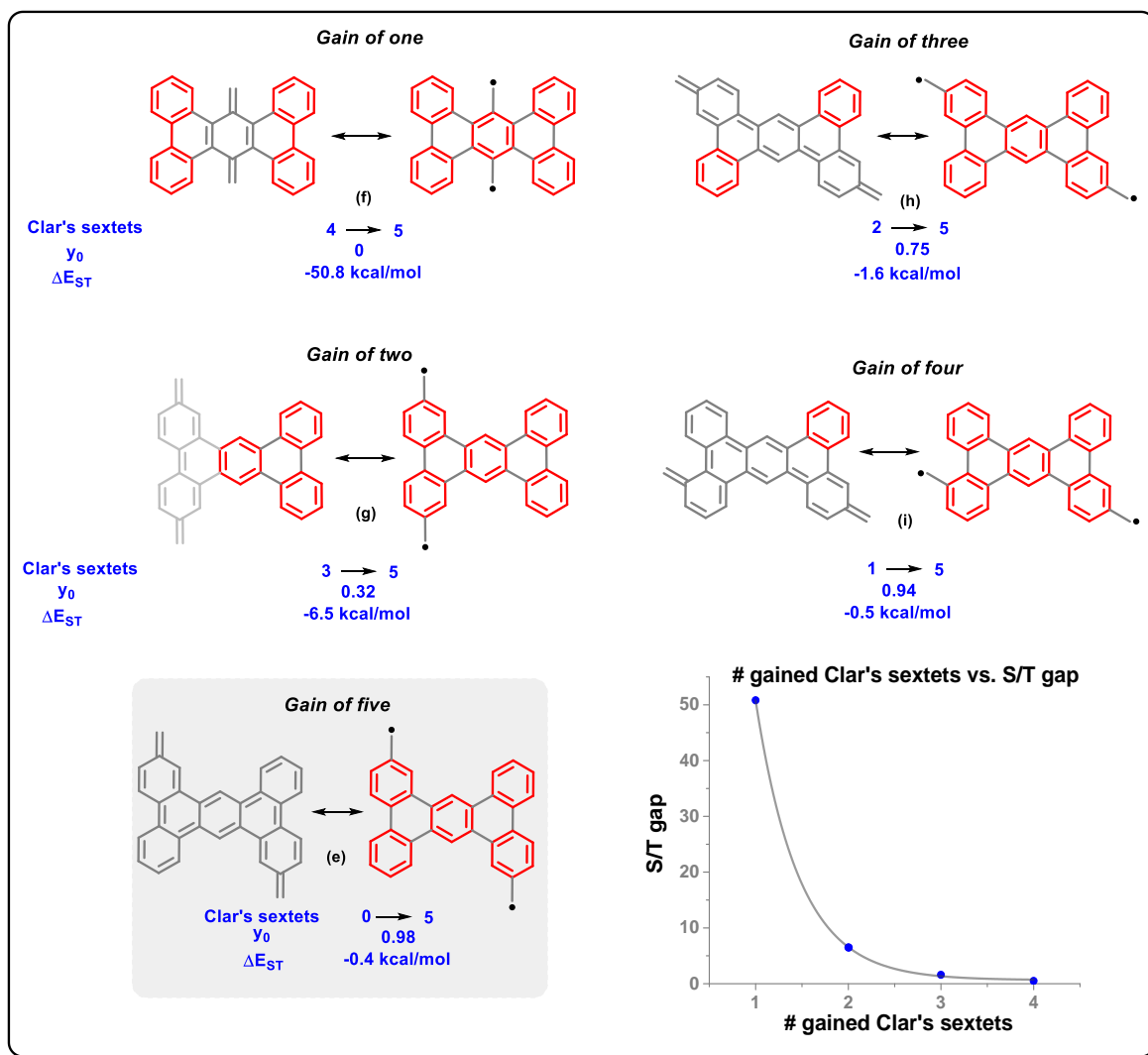


**Figure 4.** Selected diradicals built upon the tribenzo[f,k,m]tetraphene core. Not all of the patterns based on the “ideal Clar’s systems” are equal: the gain of Clar’s sextets in the diradical form vary depending on the relative placement of the spin centers. Bottom right: the S/T gap as a function of the number of gained Clar’s sextets. Calculations are performed at (U)CAM-B3LYP/6-31G(d,p) level of theory

Furthermore, one can expand the “ideal systems” by a number of additional design elements such as conjugating side chains or fused rings as illustrated in Figure 5. The parent system with the two methylene radicals (the Kekulé diradical **e**) already has high diradical character of  $y_0 = 0.98$  and S-T gap of -0.4 kcal/mol. Extending conjugation at the radical centers, e.g., by adding either a double bond or a benzene ring, can further stabilize the radicals. By adding two more phenyl rings, one can amplify the effect even more. This change increases the diradical character to  $y_0 = 1.00$  for **I** and decreases the S-T gap of **I** to zero. The nearly perfect diradical character can be explained by the gain of **seven** Clar’s sextets in the open-shell form relative to the closed shell configuration with **zero** Clar’s sextets. Interestingly, **p** and **I** have one Clar’s sextet more than tribenzo[f,k,m]tetraphene. By following this diradical evolution process, we have

reached a point where we made two perfect diradicals, one Kekulé and one non-Kekulé, i.e., **p** and **l**. Now, the question is what are the practically accessible versions of these systems. One can extend the pattern to cyclic diradicals **m** and **q**, but still has a resonance structure where radical center is outside the cycle. If we fuse an additional cycle at this position, we reach our target fully cyclic Kekulé, **K**, and non-Kekulé, **NK**, structures where a high degree of diradical character is preserved (center of figure 5).

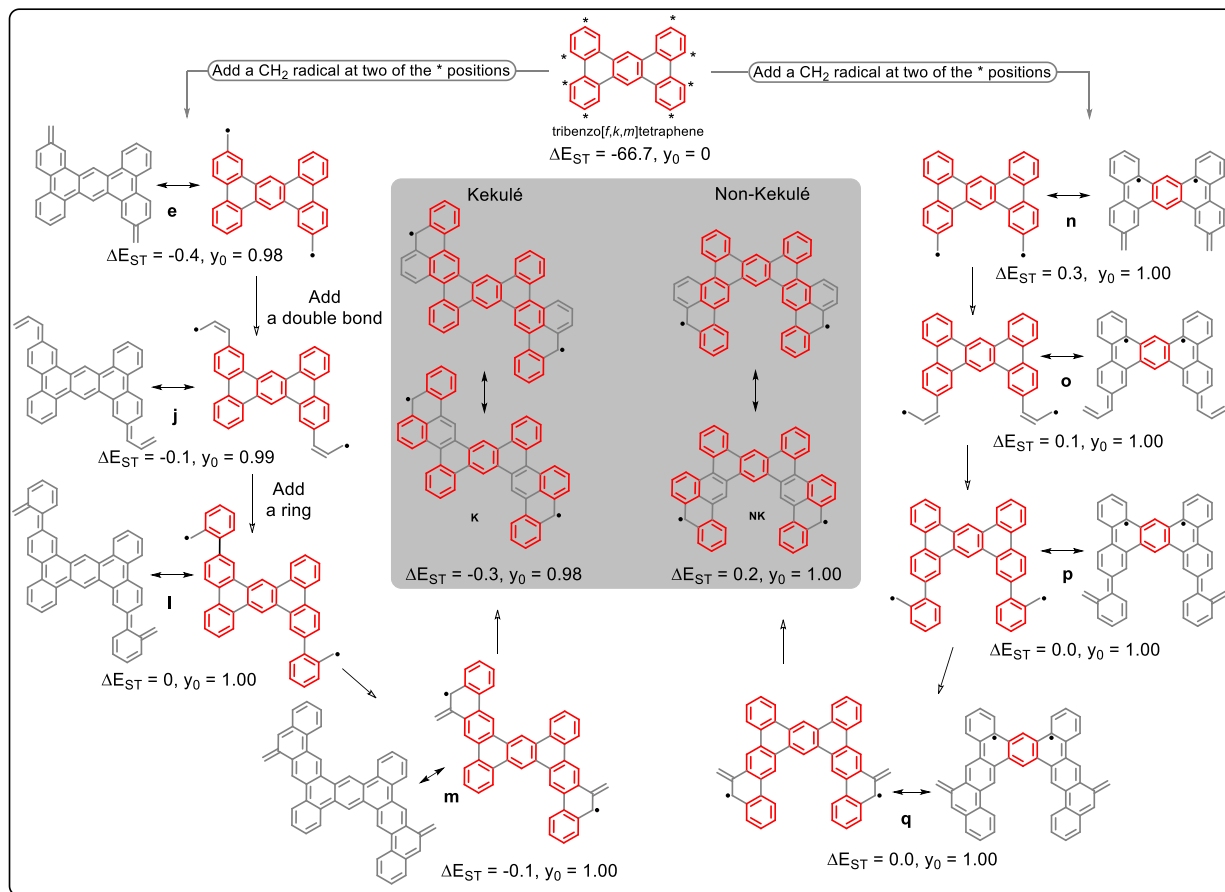


**Figure 5.** Extending the parent tribenzo[f,k,m]tetraphene framework to our Kekulé and non-Kekulé system. Calculations are performed at (U)CAM-B3LYP/6-31G(d,p) level of theory

### The non-Kekulé alternatives

As one can see from Figure 5 and the SI, this general design concept also offers a number of non-Kekulé diradicals. One of the non-Kekulé structures which is close structurally to the target Kekulé radical is highlighted in the right part of Figure 5. We thought that this parallel design can provide a valuable opportunity to compare the two types of diradicals side-by-side. Non-Kekulé diradicaloids have high spin (triplet) ground state which makes them extremely reactive and renders their solution synthesis very challenging. One of the most studied non-Kekulé diradicaloids is triangulene (Clar's hydrocarbon) which is the smallest triplet-ground state PAH. Most of the initial solution based synthesis of triangulene resulted in



polymerization of the formed diradicaloid.<sup>53,54</sup> The triplet ground state of triangulene was confirmed by Nakasuji and coworkers where they made 2,6,10-tri-*tert*-butyltriangulene.<sup>55</sup> However, since the *tert*-butyl groups were not placed at positions of highest spin density, the compound easily got polymerized. Recently, Gross and coworkers reported an on-surface synthesis of unsubstituted triangulene. A combination of scanning tunneling and atomic force microscopy (STM/AFM) was used to dehydrogenate the precursor molecules to get the product triangulene.<sup>56</sup> While we were preparing this manuscript, Arikawa et al. reported the solution synthesis and isolation of crystalline triangulene. The introduction of bulky substituents to the reactive zig-zag edges helps to kinetically stabilize the diradical and triplet ground state was confirmed by electron paramagnetic resonance studies.<sup>57</sup> Wu and coworkers reported first persistent triplet diradicaloid, 1,14:11,12-dibenzopentacene in solution. The persistence of this triplet diradicaloid below -78 °C was ascribed to the kinetic blocking of most reactive sites and to the large extend of spin delocalization in molecular framework. Although, the triplet ground state was confirmed by ESR measurements, the compound was stable in solution only under -78 °C and inert atmosphere. So, the search for stable non-Kekulé diradicaloids continues (Figure 2).<sup>58</sup>

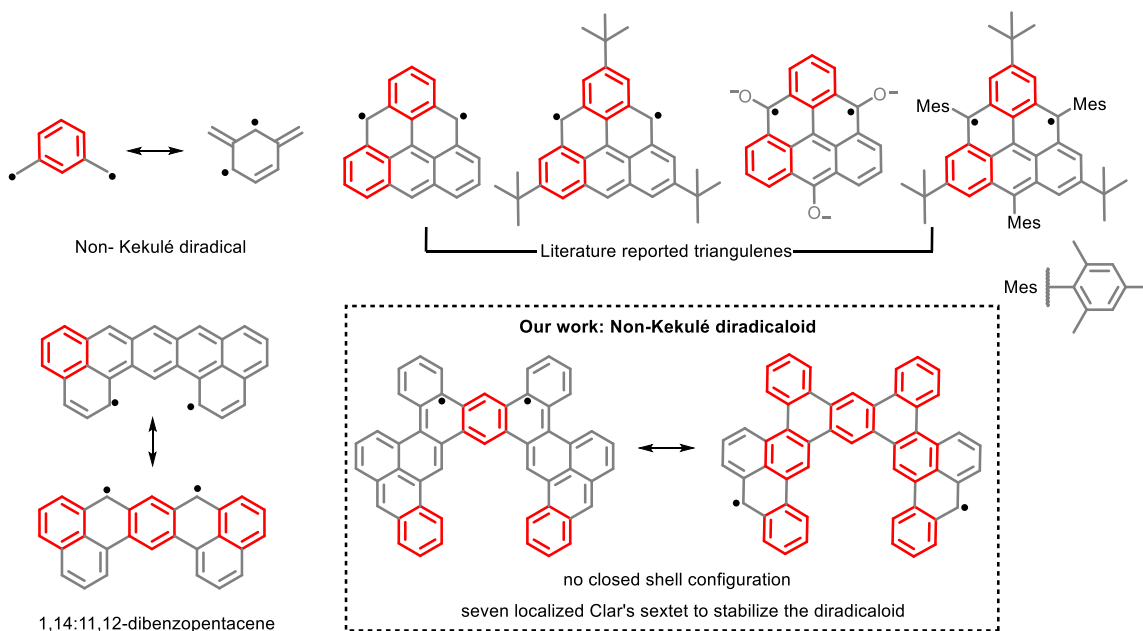


**Figure 6.** Various non-Kekulé structures from the literature in comparison to the system presented in our work

### The advantage of peri-annulations

Synthesis of extended polyaromatics often provides interesting synthetic challenges that spans innovation.<sup>59–86</sup> In the present case, an attractive synthetic route to diradicaloids is opened by our recent work on radical alkyne *peri*-annulations (i.e., “zigzag annulations”)<sup>87–89</sup> where we developed a new strategy for expanding the scope of  $\pi$ -annulations at zig-zag edge of PAHs. Fortuitously, the *peri*-cyclizations provide

the necessary pieces for accomplishing the synthesis of new diradicals in a concise and modular fashion. In particular, this reaction provides functionalized benzantrones which can be considered as masked phenalenyl radical with an extra localized Clar's sextet. These pieces can be fused, like Legos, into larger structures where, by changing starting materials, we can control the associated characteristics and properties and fine-tune the properties of diradical graphene fragments. For example, if the two benzantrone units are connected in a head to tail fashion using a phenyl linker by a sequence of cross coupling and C-H activation steps, the resulting system can be converted into a Kekulé diradicaloid. The resulting Kekulé diradicaloid will be electronically stabilized in the open shell configuration by seven localized Clar's aromatic sextets as opposed to two Clar's sextets in the closed-shell configuration. On the other hand, connecting the two benzantrone units in head-to-head fashion creates the non- Kekulé diradicaloid. The latter is also stabilized by seven localized Clar's sextets but lacks a spin-paired closed shell resonance structure. (Figure 7)

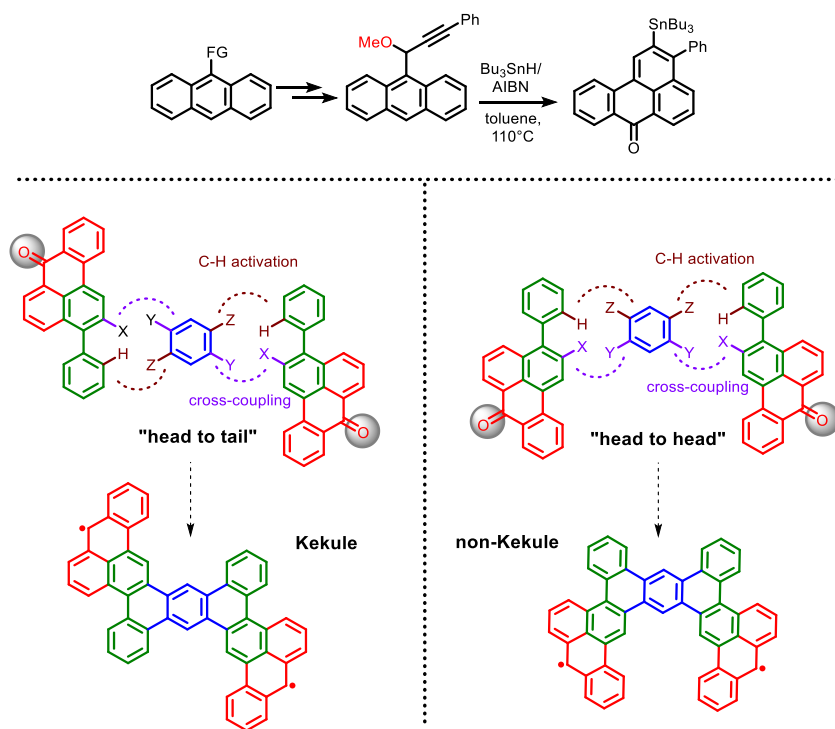


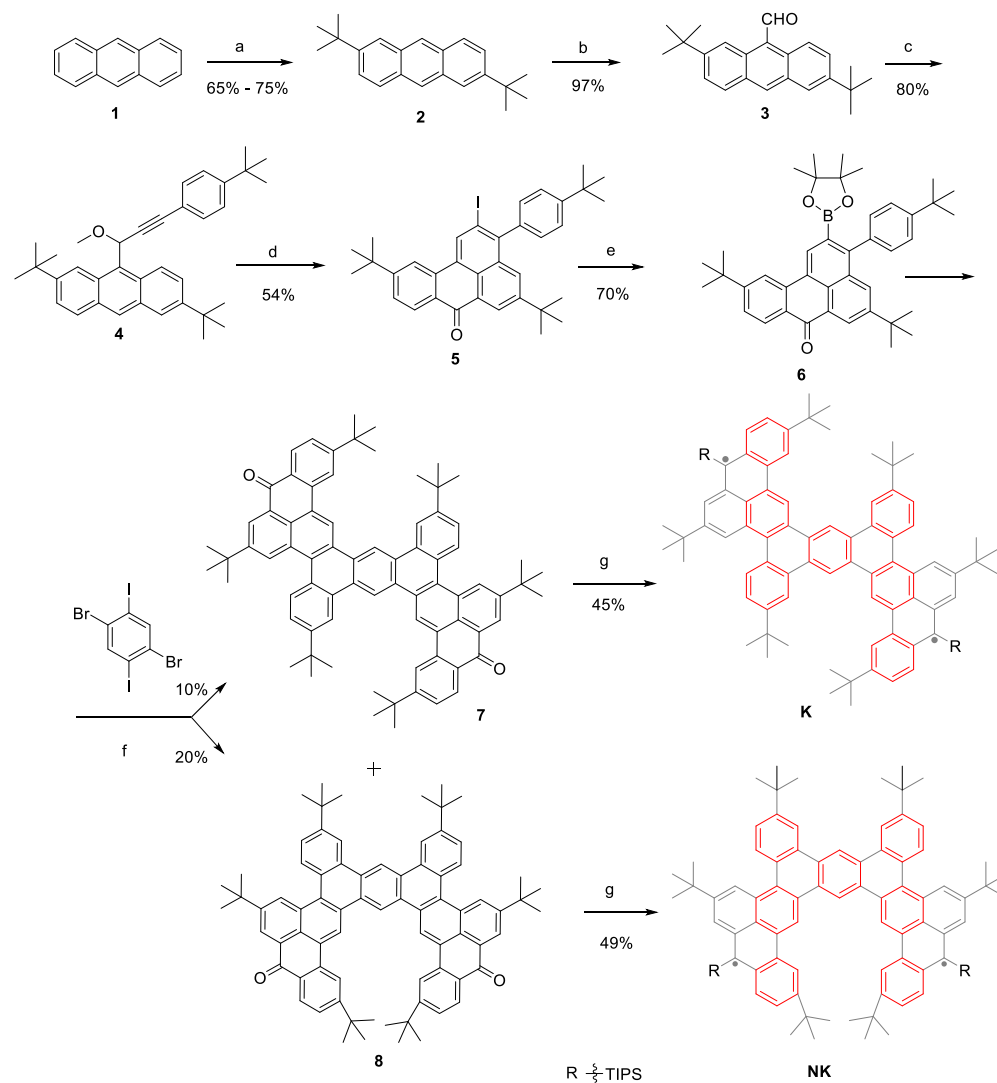
**Figure 7.** a) General scheme for peri-annulations. B) Synthetic design of diradicaloids

Herein, we report a Kekulé diradicaloid with high diradical character (0.98) and reasonable kinetical stability (half lifetime ~ 42 h) and compare its properties with an isomeric non- Kekulé diradicaloid with a half lifetime of 2 h. This comparison shows that a Kekulé structure, where electron pairing is possible, can with the help of Clar's sextets rival the analogous non-Kekulé structure in the degree of diradical character and stability.

## Synthesis

The synthesis started with introduction of *t*-butyl groups to anthracene to yield 2,6-di-*tert*-butylanthracene, **2**, to increase the solubility and kinetic stability of the polyaromatic target products. Formylation at the ninth position of 2,6-di-*tert*-butylanthracene yielded compound **3** in high yield. Addition of 4-*tert*-butylphenyl acetylide to 2,6-di-*tert*-butylanthracene-9-carbaldehyde, followed by in situ reaction with methyl iodide, gives the propargylic ether precursor **4** for the radical cyclization in 80% yield. The iodo-substituted benzanthrone product **5** is formed in the overall 54% yield after the subsequent Bu<sub>3</sub>Sn-mediated radical cyclization, iodination and oxidation. The cyclization is the key step that enabled us to get functionalized precursors for the following assembly of the final polyaromatic system. Borylation of compound **5** yielded **6** in 70% yield.

Compound **6** is subjected to the one-pot Pd-catalyzed Suzuki coupling and dehydrohalogenation sequence with 1,4-dibromo-2,5-diiodobenzene to form the mixture of the two target polyaromatic diketones **7** and **8** in 10% and 20% isolated yields, respectively. Although formation of the Kekulé precursor can be rationalized by the sequence of Suzuki reaction at the iodo-substituted positions and C-H/C-Br coupling, the formation of isomeric head-to-head dimer suggests that the mechanistic picture is likely to be more interesting and complex. Although the reaction mechanism is not clear, one can speculate that it involves a benzyne intermediate (see the SI).



**Scheme 1:** Synthesis: (a) *t*BuOH, TFA, reflux, 16h; (b) CHCl<sub>2</sub>OMe, TiCl<sub>4</sub>, DCM, 0 °C – reflux, 1 h; (c) 1. *tert*-butylPhCCH, *n*-BuLi, THF, -78 °C – rt, 3 h; 2. MeI, rt, 12h; (d) 1. Bu<sub>3</sub>SnH (2 equiv.), AIBN (1 equiv.) Toluene, 110 °C, 18 h; 2. I<sub>2</sub>, DCM, rt, 2 h; 3. DDQ, DCM, rt, 2 h; (e) Bis(pinacolato)diboron, Pd(dppf)Cl<sub>2</sub>, DMF, KOAc, 80°C, 6 h; (f) 1. Pd(PPh<sub>3</sub>)<sub>4</sub> (0.2 equiv.), K<sub>2</sub>CO<sub>3</sub> (5 equiv.), 18-crown-6 (0.2 equiv.), Toluene/H<sub>2</sub>O (4:1), 100 °C, 18 h; 2. Pd(PCy<sub>3</sub>)<sub>2</sub>Cl<sub>2</sub> (0.2 equiv.), Pivalic acid (0.2 equiv.), Cs<sub>2</sub>CO<sub>3</sub> (5 equiv.), reflux, 20 h; (g) 1. TIPSCCH, *n*-BuLi, THF, -78° C – rt; 2. SnCl<sub>2</sub>, 0° C - rt

Due to the presence of the six *t*-butyl groups attached to the core, the diketones are soluble in various organic solvents and could be crystallized to provide suitable samples for X-ray crystallography. The *t*-butyl groups also serve as a steric bulk to stabilize the final diradicaloids. Subsequent addition of TIPS-acetylide and reduction with SnCl<sub>2</sub> provided fully deoxygenated polyaromatic diradicaloids **K** (“Kekulé”) and **NK** (“Non-Kekulé”) in moderate yields.

Both diradicaloids **K** and **NK** are purified on a silica gel column deactivated by triethylamine. **K** has a reasonably long half-lifetime of 42 hours in dichloromethane (DCM) under ambient air and light. Interestingly, its triplet counterpart, **NK**, has a noticeably shorter lifetime of 2 hours in DCM under ambient light and air. Both **K** and **NK** are NMR silent at the room temperature which is consistent with their paramagnetic character.

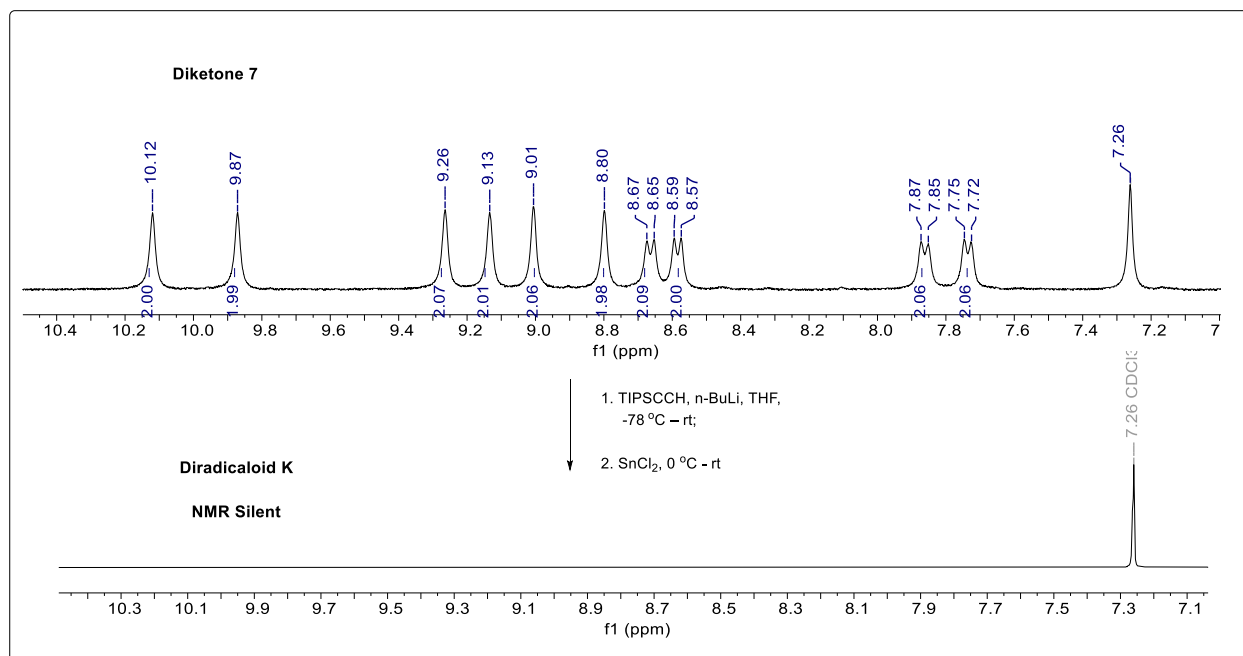


**Figure 8:** Comparison of <sup>1</sup>H NMR spectra of diradicaloid **K** and its precursor diketone **7**.

**Crystal Structure:** Although we have been unable to obtain single crystals of both **K** and **NK** due to intrinsic instability of these diradicaloids, we carried out crystallographic analysis on single crystals of the precursor diketones **7** and **8** that were grown by slow diffusion of methanol into a dichloromethane solution of **7** or **8**. Compound **7** crystallizes in a monoclinic space group *P2<sub>1</sub>/c*, with the asymmetric unit containing one and a half molecule of **7** and one interstitial dichloromethane molecule (Figure 9a). Fitting a least-square plane only through 52 cyclic C atoms of each [4]helicene shows that one of the molecules is substantially more distorted from planarity than the other, with the sums of squared atom-to-plane distances equal to 32.6 Å<sup>2</sup> and 12.9 Å<sup>2</sup> and the corresponding distances varying from -1.037 Å to 1.843 Å and from -1.016 Å to +1.016 Å, respectively (the negative and positive signs indicate atoms arranged on opposite sides of the plane). In the less distorted [4]helicene, the two halves of the molecule are related by a crystallographic inversion center. Examination of the crystal packing reveals extensive intermolecular  $\pi$ - $\pi$  interactions that result in chains of molecules along the *a* axis (Figure 9b). The interactions between these chains are relatively weaker.

Compound **8** crystallizes in an orthorhombic space group *Pbca*. The asymmetric unit contains only one [4]helicene molecule (Figure 9c). Steric repulsion between the terminal t-butyl groups in **8** accounts for a much greater local distortion from planarity. The dihedral angle between the planes passing through the central ring and the terminal ring is 48.0°. Interestingly, however, a least-squares plane fit through the 52 cyclic C atoms gives the sum of squared atom-to-plane distances equal to 34.8 Å<sup>2</sup>, which is only slightly larger than the value of 32.6 Å<sup>2</sup> calculated for the more distorted [4]helicene molecule in the crystal structure of **7**. Nevertheless, the atom-to-plane distances in molecule **8** vary in a notably greater range, from -2.375 Å to 2.355 Å. These observations indicate that the peripheral regions of **8** are relatively flat, which explains the similarity of the sum of least-squares deviations to that observed for the more distorted molecule in the crystal structure of **7**. This relative flatness of the peripheral regions of **8** provides for an efficient crystal packing, in which molecules are arranged in layers parallel to the *ac* plane of the lattice. Within the layers, the molecules are organized in columns due to intermolecular  $\pi$ - $\pi$  interactions (Figure 9d), and the molecules from neighboring columns interact with each other via weaker  $\sigma$ - $\pi$  contacts.

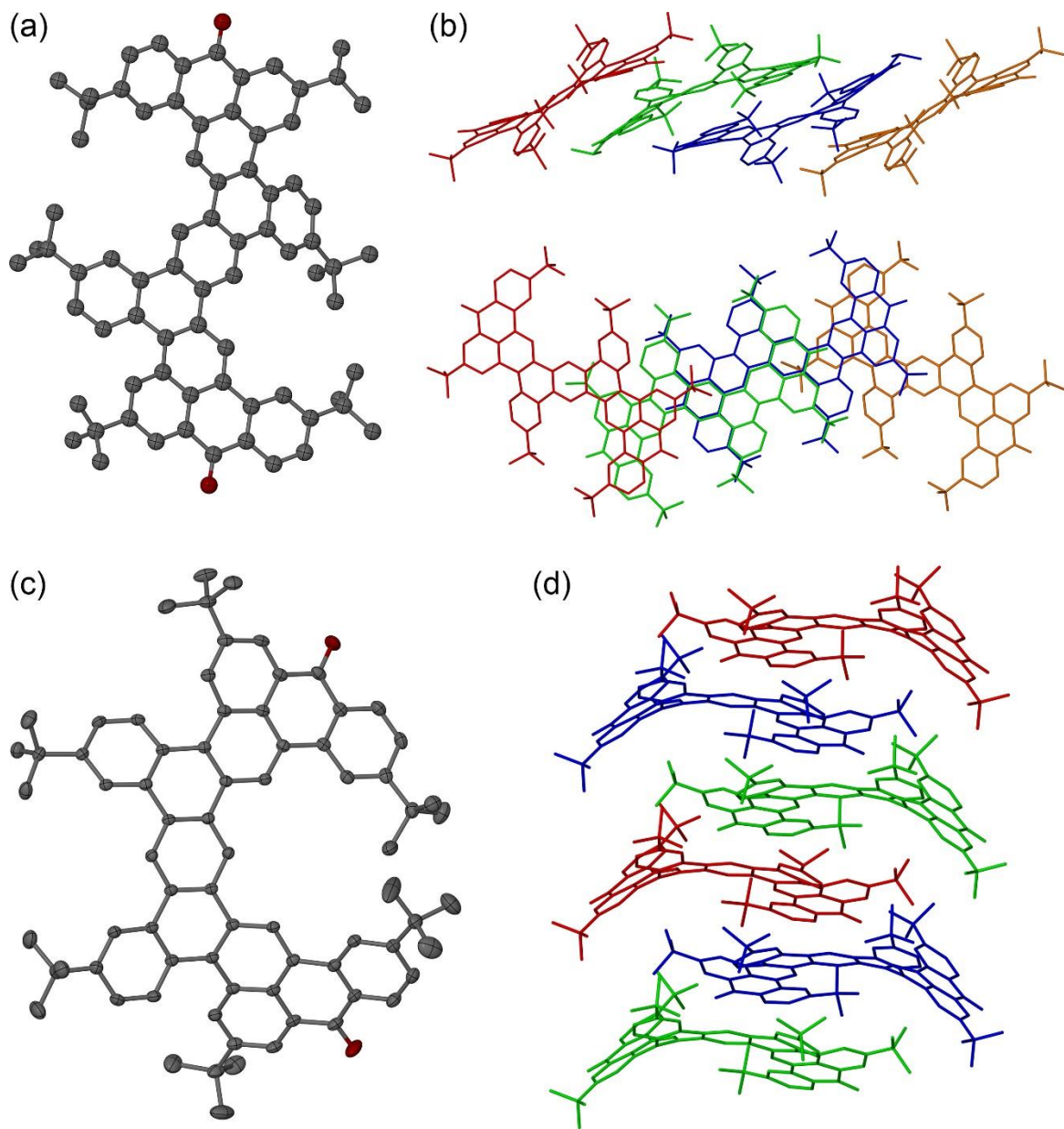


**Figure 9.** The thermal ellipsoid plot of a one of the [4]helicene molecules in the asymmetric unit of **7** (a) and the side and top views of molecular chains in the crystal packing of **7** (b). The thermal ellipsoid plot of the asymmetric unit of **8** (c) and the side view of the molecular chain in the crystal packing of **8** (d).

### Photophysical properties

The diketones **7** and **8** are yellow powders that give greenish yellow solutions in dichloromethane. Both show similar absorption spectra with the lowest energy absorption peak at 456 nm. Interestingly, compound **7** has a ~2-fold greater extinction coefficient than **8** ( $3.1$  vs  $1.8 \times 10^4 \text{ mol}^{-1} \text{ L cm}^{-1}$  at 456 nm), presumably due to the differences in molecular symmetry. Both compounds **7** and **8** have featureless fluorescent spectra

with the emission maxima at 512 nm and 518 nm, respectively. The two diketones are highly fluorescent with relatively high quantum yields (QY) (0.87 for **7** and 0.80 for **8**). (Figure 10)

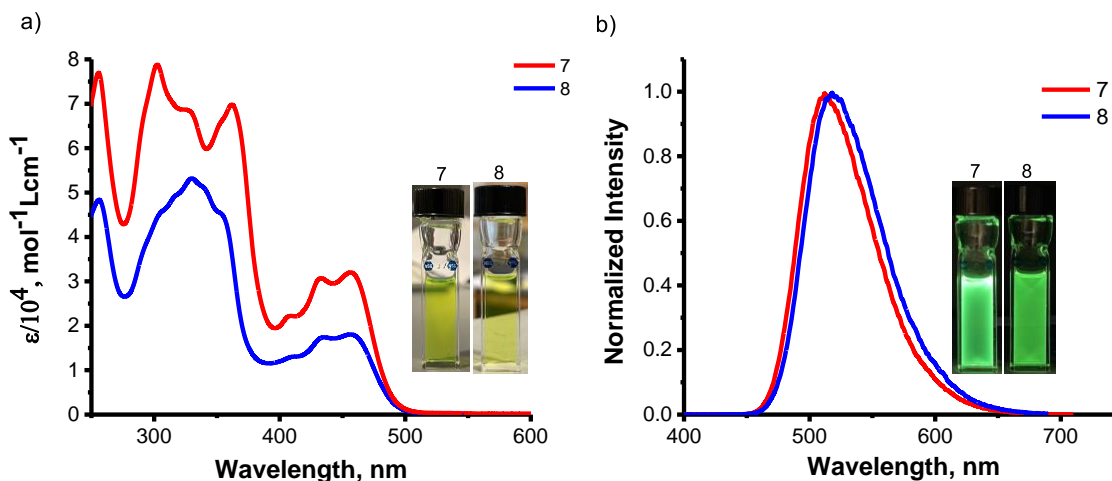


**Figure 10.** (a) Shows absorption spectra of diketones **7** and **8** in dichloromethane (the pictures of **7** and **8** in dichloromethane are shown as well). (b) Shows emission spectra diketones **7** and **8** in dichloromethane (pictures of **7** and **8** under UV (365 nm) is shown as well).

Conversion of diketones **7** and **8** into diradicals **K** and **NK** leads to bathochromic shift in absorbance. Both compounds **K** and **NK** are red powders and give red colored solutions in dichloromethane. The two molecules show similar features in the absorption spectrum - the lowest energy peaks at 527 nm and 460 nm for **NK** vs. 529 nm and 467 nm for **K**. Additionally, **K** also has two very weak absorptions at 704 nm and 780 nm. These two lower energy bands are similar in energy to the low-lying singlet excited states typical for singlet diradicaloids and suggested to originate from a doubly excited electronic configuration (H,H  $\rightarrow$  L,L) (H: HOMO; L: LUMO).<sup>90</sup> Such transitions may be another manifestation of the hidden zwitter-ionic character of singlet diradicals<sup>91</sup>. **NK** also shows two lower energy bands at 594 nm and 785 nm. It could be either due to doubly excited electronic configuration (H,H  $\rightarrow$  L,L) or due to small amount of impurities. (Figure 11).



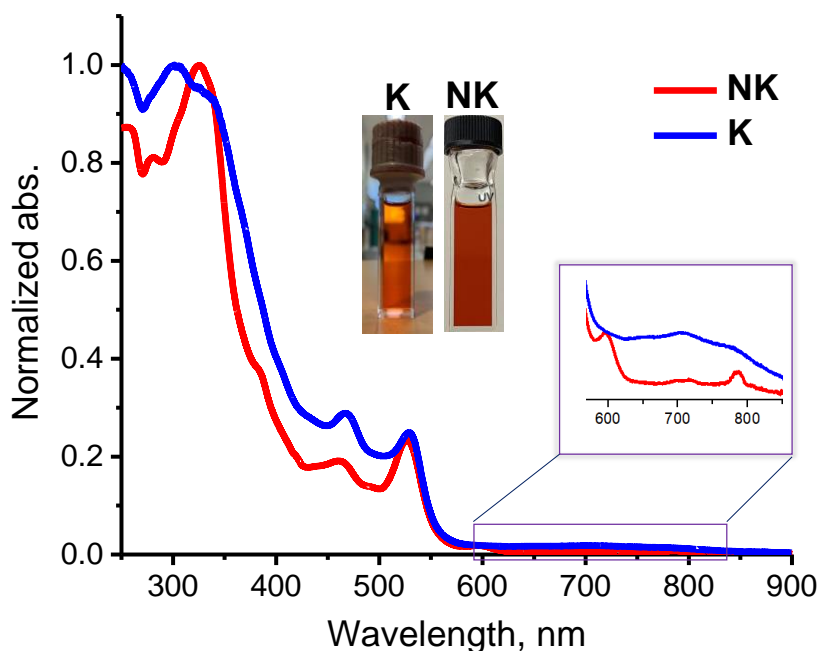


**Figure 11.** Absorption spectra of K and NK in dichloromethane.

**Cyclic Voltammetry:** Cyclic voltammetry and differential pulse voltammetry measurements for both compounds **K** and **NK** (1 mg/ml) were recorded by scanning the potential from -1.4 to 0.5 V (vs. Ag/Ag<sup>+</sup>) at a scan rate of 0.05 V s<sup>-1</sup> (Figure 12). The CVs of the two compounds recorded in DCM each exhibit two redox couples, which are electrochemically quasi-reversible as evidenced by their peak-to-peak separations ( $\Delta E_p$  in Table 1). For each compound, we have named the process occurring at the more oxidizing potential as “ox” and the process occurring at the more reducing potential as “red.” The values of the half wave potentials for the two processes are  $E_{1/2}^{ox} = -0.15$  V and  $E_{1/2}^{red} = -1.32$  V. “The DPV measurements are also consistent with CV measurements, in that a peak is evident at the stated half wave potentials.

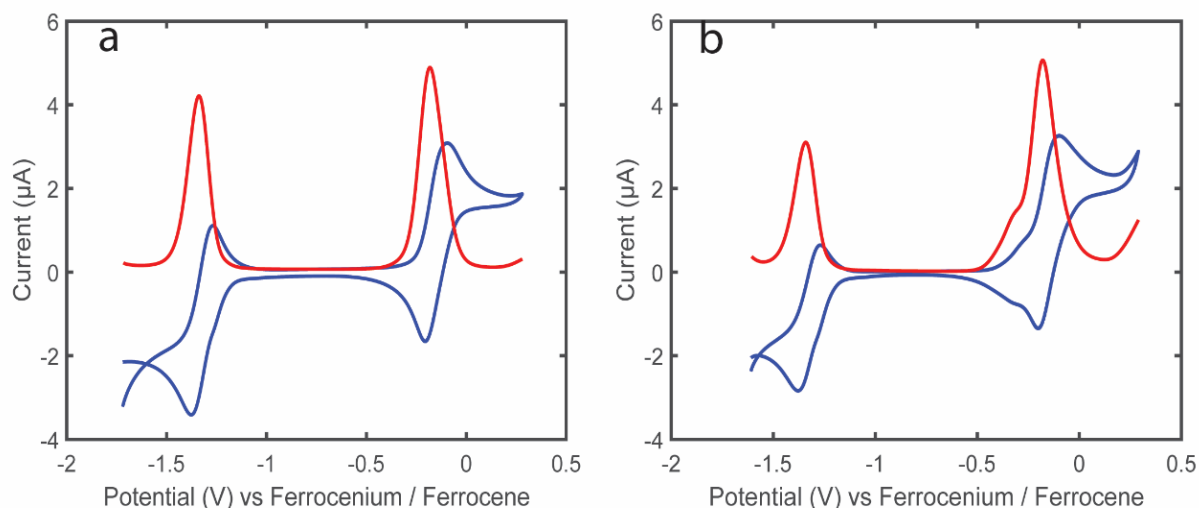


**Figure 12:** Cyclic voltammograms (blue) and differential pulse voltammograms (red) of compounds **K** (a) and **NK** (b) in DCM with 100 mM NBu<sub>4</sub>PF<sub>4</sub>.

The results of the electrochemical investigations are summarized in Table 1. The “HOMO/LUMO” energy levels of both compounds are nearly identical. They were calculated (-4.54 and -3.60 eV, respectively) from the onset potential of the oxidation ( $E_{\text{ox}}^{\text{onset}}$ ) and reduction ( $E_{\text{red}}^{\text{onset}}$ ) processes according to the following equations: HOMO =  $-(4.8 + E_{\text{ox}}^{\text{onset}})$  eV and LUMO =  $-(4.8 + E_{\text{red}}^{\text{onset}})$  eV.<sup>92</sup> The current crossover on the CVs for both compounds at potential < -1.5 V arises as the scan started in the diffusion-limited region. Electrochemical measurements suggest that oxidation and reduction proceed as two-electron ( $E^1_{\text{ox}} = E^2_{\text{ox}}$  and  $E^1_{\text{red}} = E^2_{\text{red}}$ ) processes rather than two one-electron processes since the one-electron Fc/Fc<sup>+</sup> redox couple (used as the internal reference) has approximately double the peak-to-peak separation. This scenario is possible for systems with two degenerate molecular orbitals.<sup>57</sup>

**Table 1:** Electrochemical parameters determined from the CVs<sup>a</sup>

Sample	$E_{1/2}^{\text{ox}} / \text{V}$	$E_{1/2}^{\text{red}} / \text{V}$	$E_{\text{ox}}^{\text{onset}} / \text{V}$	$E_{\text{red}}^{\text{onset}} / \text{V}$	$\Delta E_p (\text{ox}) / \text{mV}$	$\Delta E_p (\text{red}) / \text{mV}$	HOMO / eV	LUMO / eV
K	-0.15	-1.32	-0.26	-1.20	105	110.1	-4.54	-3.60
NK	-0.15	-1.32	-0.26	-1.20	109	106.8	-4.54	-3.60

<sup>a</sup>The onset potentials were determined using the intersection of asymptotic lines from the baseline current preceding the redox wave, and the increasing current at the fast-rising portion of the redox wave.

**Magnetic Properties:** Magnetic behavior of **K** and **NK** was further probed by variable temperature (VT) electron paramagnetic resonance (EPR) on the powder samples of the two diradicaloids. The two compounds show opposite behavior, as expected from the differences in their ground states (singlet for **K** and triplet for **NK**). (Figure 13)

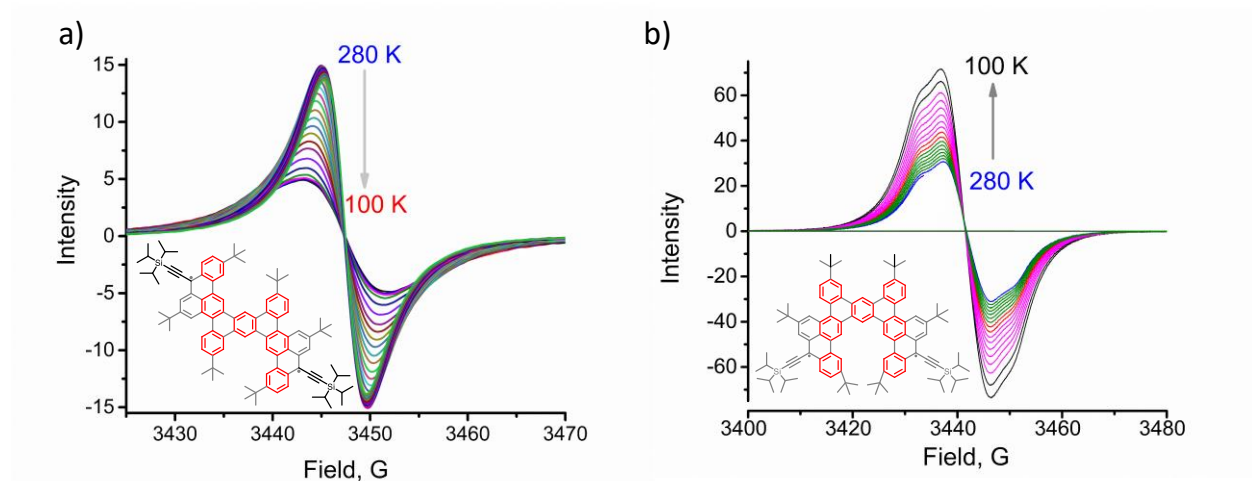


**Figure 13.** Variable Temperature (VT) solid-state EPR data of (a) **K** and (b) **NK**.

Variable-temperature magnetic measurements on a powder sample of **K** revealed that the product of molar magnetic susceptibility ( $\chi$ ) by temperature decreases linearly as a function of temperature (Figure 14). This dependence was fit to a modified Bleaney-Bowers equation,

$$\chi T = \frac{2N_A\mu_B^2g^2}{k_B(3 + e^{-\Delta/kT})} + \chi_{TIP}T$$

where  $N_A$  is Avogadro's number,  $\mu_B$  is the Bohr magneton,  $k_B$  is the Boltzmann constant, and  $\chi_{TIP}$  is a temperature-independent paramagnetic contribution (due to a minor unidentified impurity). The fitting procedure gave a singlet-triplet energy gap ( $\Delta$ ) of -0.8 kcal/mol. Unfortunately, we were unable to achieve reliable magnetic measurements on a sample of **NK** due to its lower stability and much shorter lifetime.

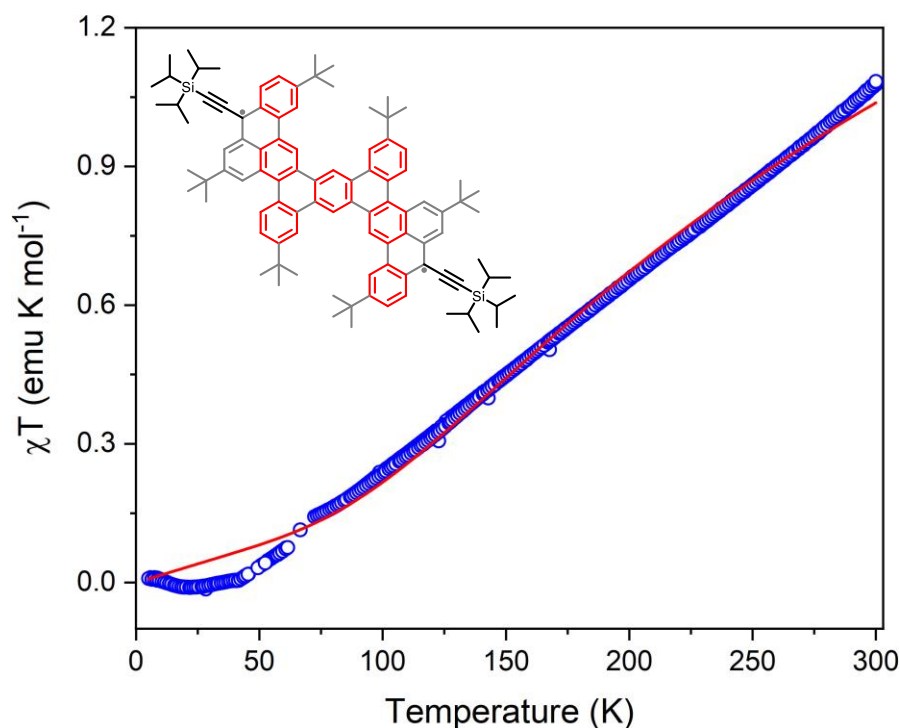


**Figure 14.** The temperature dependence of the  $\chi T$  product for a powder sample of **K**. The solid red line indicates the fit to the Bleaney-Bowers equation (see the text).

**Computations:** To understand the singlet and triplet ground state of **K** and **NK** respectively, we did calculations on the respective core structures. The degree of diradical character ( $y_0$ ) for singlet diradicaloid **K** was estimated from the electron occupancies of frontier natural orbitals using Yamaguchi's scheme at the UCAM-B3LYP/6-31G(d,p) level of theory. The computations produced a very high  $y_0$  value of 0.98. It was also calculated that **K** has a small S-T gap of  $\Delta E_{S-T} = -0.3$  kcal/mol while **NK** has an equally small S-T gap of  $\Delta E_{S-T} = +0.2$  kcal/mol. Although **K** is a ground state singlet while **NK** is a ground state triplet, the difference between the two states in both of these systems is very small, explaining the absence of NMR signals at room temperature.

The high diradical character of **K** can be explained from the gain of additional five Clar's sextet when going from closed-shell to open-shell configurations i.e.; two Clar's aromatic sextets in closed shell form to seven Clar's sextets in the open shell form. It is also consistent with the results from NICS(1)<sub>zz</sub> scans.<sup>94,95</sup> The scan showed larger negative NICS(1)<sub>zz</sub> for the seven localized aromatic sextets in Figure 15a. Similar results are found for **NK** where the NICS(1)<sub>zz</sub> scan also shows seven localized aromatic sextets (Figure 15b). The perfect localization of the Clar's sextets is partially compromised in the vicinity of the radical centers because the delocalization of radical is a powerful force that influences the electronic structures of the adjacent  $\pi$ -rings. One can think about this substructure as the phenalenyl subunit embedded into a polyaromatic framework. This observation illustrates both the power and the limitations of the Clar's localized aromaticity approach to the control of the electronic structure of extended polyaromatics.

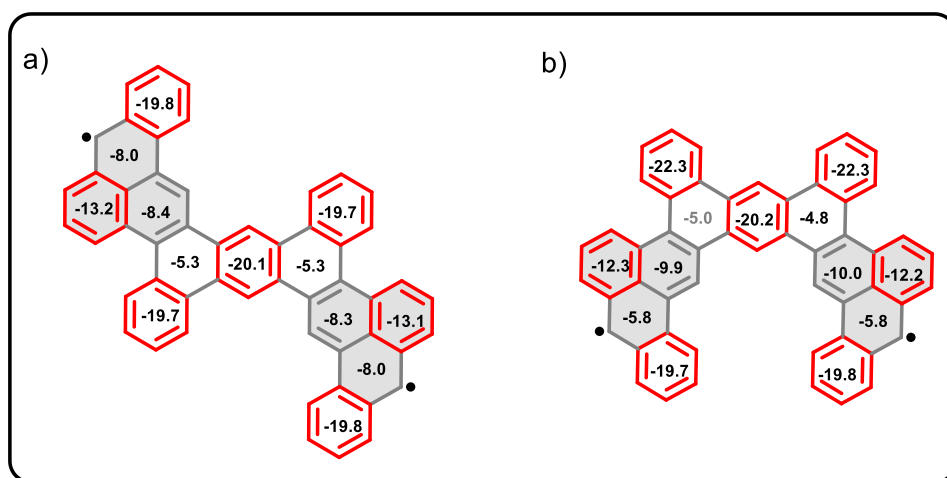


**Figure 15.** NICS(1) values of core structures of **K** (a) and **NK** (b). Calculations are performed at (U)B3LYP/6-311++g(d,p) level of theory

The NICS values are also consistent with the radical delocalization patterns revealed by the nature of singly occupied molecular orbitals (SOMOs) of the two diradicaloids. The singlet state of the Kekulé diradical **K** displayed a typical disjoint character with unpaired electrons with alpha and beta spins delocalized over different atoms (Figure 16). On the other hand, the SOMOs of the ground state of the non-Kekulé system **NK** illustrate a non-disjoint character (Figure 17). However, these differences have to do more with the singlet vs. triplet nature of the lowest states rather than with their Kekulé vs. non-Kekulé nature as confirmed by the non-disjoint diradical character of the triplet Kekulé system and the disjoint nature of the singlet non-Kekulé system.

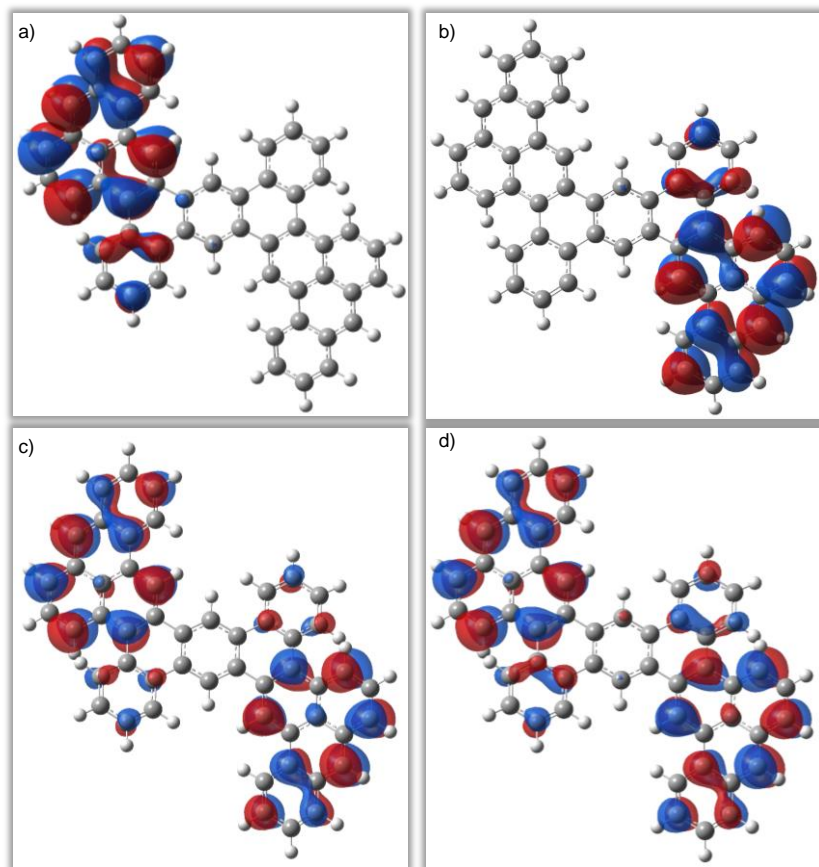


**Figure 16.** Singly occupied molecular orbitals (SOMOs) of the core structure of Kekulé diradicaloid **K**. Top: singlet ground state - alpha (a) and beta (b) spin. Bottom: triplet state - (c) alpha and beta (d) spins. Calculations are performed at CAM-B3LYP/6-31g(d,p) level of theory.

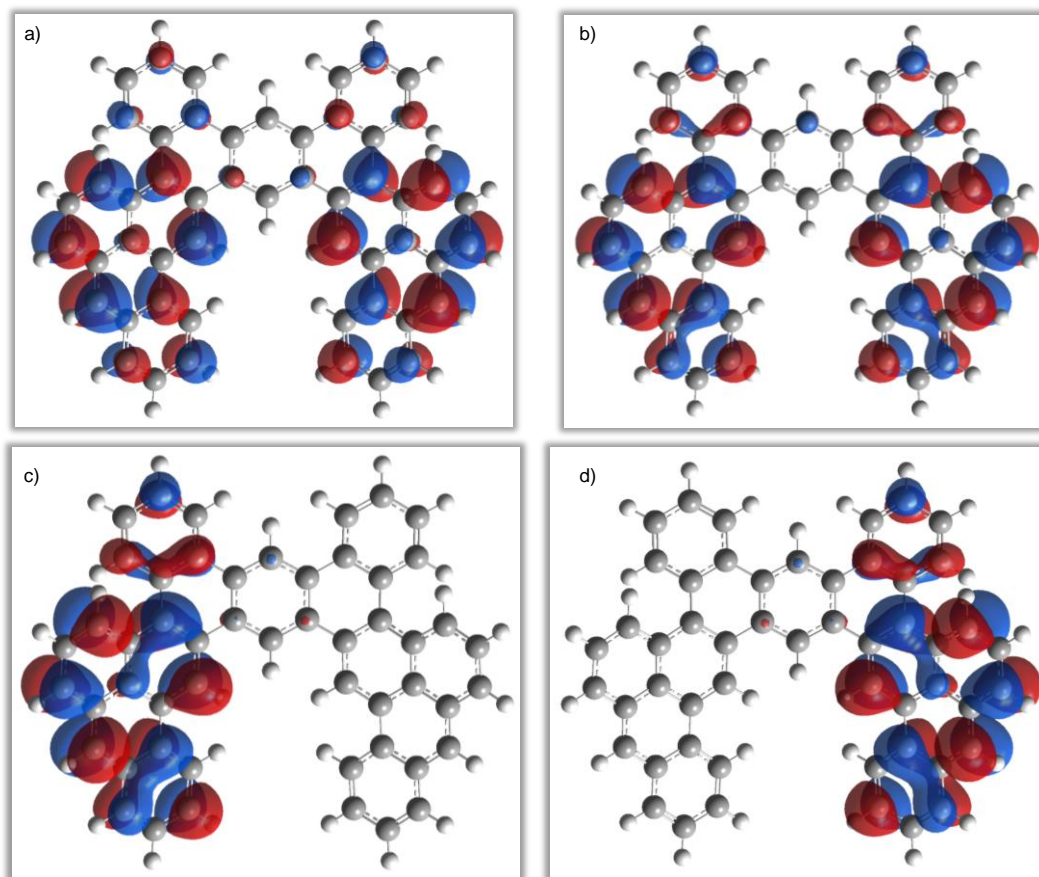


**Figure 17.** Singly occupied molecular orbitals (SOMOs) of the core structure of the non-Kekulé diradicaloid **NK**. Top: triplet ground state - alpha (a) and beta (b) spin. Bottom: singlet state - (c) alpha and beta (d) spins. Calculations are performed at CAM-B3LYP/6-31g(d,p) level of theory.

This distribution of spin density is consistent with the dominant diradical resonance structures shown in Figure 15 with little radical density at central rings that correspond to the perfect Clar's sextets and at the armchair edges. In other words, we see two benzophenalenyl radicals separated by an insulating bridge

This behavior paves the way to the emergence of spin states at the zigzag edges of larger carbon nanostructures.<sup>96-100</sup> Overall, the spin distribution is reminiscent of two benzophenalenyl radicals separated by a para- (K) or a meta- (NK) terphenyl moiety. It is interesting how little radical density does the terphenyl core acquire – another illustration of resilience resulting from the synergy of several Clar's sextets.



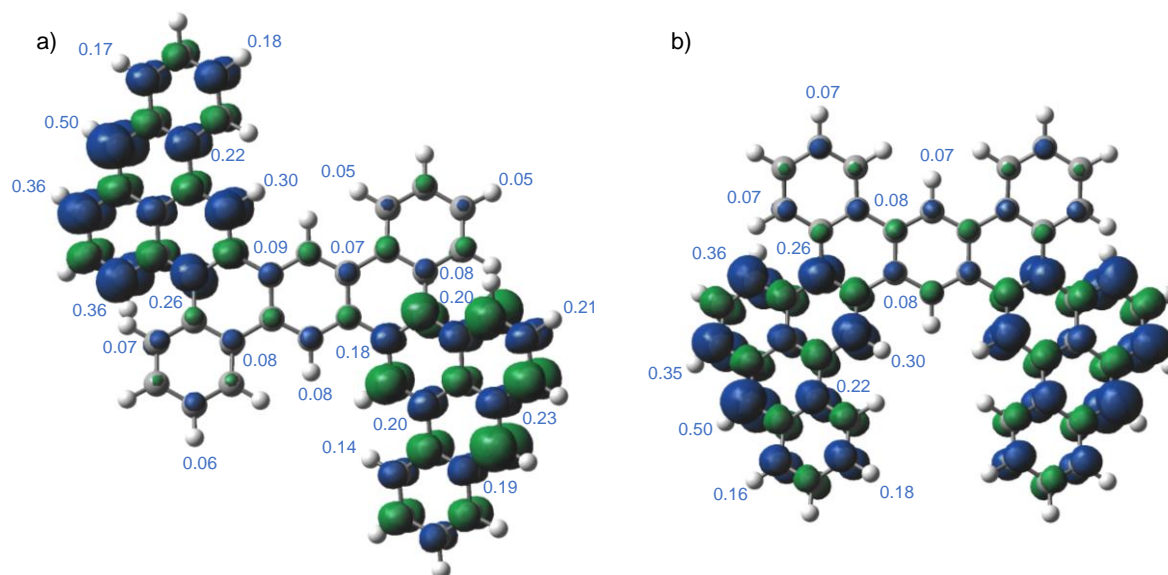


**Figure 18.** Spin densities for the core structures of Kekulé diradicaloid **K** (a) and non-Kekulé diradicaloid **NK** (b). Calculations are performed at CAM-B3LYP/6-31G(d,p) level of theory

## Conclusions

This work describes a simple and general approach to the design of new polyaromatic diradicaloids. The systematic approach starts with privileged core structures with the maximum number of Clar's sextets, and explores the electron pairing topology by addition of  $\text{CH}_2$  radicals as spin probes at different positions. Computational results clearly illustrate how, for the same core, gain of a larger number of Clar's sextets in the open-shell form increases the diradical character parameter  $y_0$  from 0 to 0.98 (where 1.0 indicates a perfect diradical).

This theoretical analysis identified two practically accessible isomeric diradicaloid topologies, one of Kekulé (**K**) type and another of non-Kekulé (**NK**) type. **K** was calculated to have very high diradical character of 0.98 and be a ground state singlet with a very low singlet triplet gap,  $\Delta E_{\text{ST}} = -0.3$  kcal/mol. **NK** was calculated to have a triplet ground state with  $y_0 = 1$  and singlet triplet gap,  $\Delta E_{\text{ST}} = 0.2$  kcal/mol.

We tested these theoretical predictions by synthesizing and characterizing isomeric tridecacyclic polyaromatic diradicaloids, **K** and **NK**. The two isomeric systems were assembled using a sequence of radical *peri*-annulations, cross-coupling and C-H activation. Both molecules are NMR-inactive but EPR-active at room temperature. The diradicals are kinetically stabilized by six *tert*-butyl substituents and (triisopropylsilyl)acetylene groups. The experimentally measured singlet-triplet energy gap ( $\Delta E_{\text{S-T}} = -0.2$  kcal/mol) in diradicaloid **K** is in a good agreement with the computational predictions. Despite having high diradical character, both molecules were stable in inert atmosphere in the absence of light. **K** was

moderately stable even in presence of air and light, with a half-lifetime of 42 h. The non-Kekulé diradical **NK** had a shorter half-lifetime of 2h.

In summary, this work illustrates how theoretical design of diradicals assisted by computations and new synthetic methods (the radical *peri*-annulation) opens synthetic access to relatively stable polyaromatics with very high diradical character. We hope that it will pave the way to the development of new types of organic magnets.

**Acknowledgment.** We are grateful to the National Science Foundation for the financial support of research at FSU (awards CHE-2102579 to I. A. and CHE-1955754 to M.S.). F.K. is grateful to Prof. Jack Saltiel and Dr. Sumesh Krishnan for letting him use their HPLC, UV-Vis and Fluorimeter instruments and to Patricia Mehaffy for the experimental assistance. F.K and I.A are grateful for helpful discussions from Prof. Jishan Wu. R.A.L is grateful to Florida State University for Start-Up funds. D.S. is grateful to Prof. Geoffrey Strouse for use of his glove box. The National High Magnetic Field Laboratory is supported by the National Science Foundation (DMR-1644779) and the State of Florida. This project also used resources provided by the X-ray Crystallography Center (FSU075000XRAY) and the Materials Characterization Laboratory (FSU075000MAC) at the FSU Department of Chemistry and Biochemistry. This work also made use of the Rigaku Synergy-S single-crystal X-ray diffractometer which was acquired through the NSF MRI program (award CHE-1828362).

## REFERENCES

- (1) Kamada, K.; Ohta, K.; Kubo, T.; Shimizu, A.; Morita, Y.; Nakasuji, K.; Kishi, R.; Ohta, S.; Furukawa, S.; Takahashi, H.; Nakano, M. Strong Two-Photon Absorption of Singlet Diradical Hydrocarbons. *Angewandte Chemie International Edition* **2007**, *46* (19), 3544–3546. <https://doi.org/10.1002/anie.200605061>.
- (2) Chikamatsu, M.; Mikami, T.; Chisaka, J.; Yoshida, Y.; Azumi, R.; Yase, K.; Shimizu, A.; Kubo, T.; Morita, Y.; Nakasuji, K. Ambipolar Organic Field-Effect Transistors Based on a Low Band Gap Semiconductor with Balanced Hole and Electron Mobilities. *Appl. Phys. Lett.* **2007**, *91* (4), 043506. <https://doi.org/10.1063/1.2766696>.
- (3) Chase, D. T.; Fix, A. G.; Kang, S. J.; Rose, B. D.; Weber, C. D.; Zhong, Y.; Zakharov, L. N.; Lonergan, M. C.; Nuckolls, C.; Haley, M. M. 6,12-Diarylindeno[1,2-b]Fluorenes: Syntheses, Photophysics, and Ambipolar OFETs. *J. Am. Chem. Soc.* **2012**, *134* (25), 10349–10352. <https://doi.org/10.1021/ja303402p>.
- (4) Lee, J.; Jadhav, P.; Reusswig, P. D.; Yost, S. R.; Thompson, N. J.; Congreve, D. N.; Hontz, E.; Van Voorhis, T.; Baldo, M. A. Singlet Exciton Fission Photovoltaics. *Acc. Chem. Res.* **2013**, *46* (6), 1300–1311. <https://doi.org/10.1021/ar300288e>.
- (5) Son, Y.-W.; Cohen, M. L.; Louie, S. G. Energy Gaps in Graphene Nanoribbons. *Phys. Rev. Lett.* **2006**, *97* (21), 216803. <https://doi.org/10.1103/PhysRevLett.97.216803>.
- (6) Jousselein-Oba, T.; Mamada, M.; Marrot, J.; Maignan, A.; Adachi, C.; Yassar, A.; Frigoli, M. Excellent Semiconductors Based on Tetracenotetracene and Pentacenopentacene: From Stable Closed-Shell to Singlet Open-Shell. *J. Am. Chem. Soc.* **2019**, *141* (23), 9373–9381. <https://doi.org/10.1021/jacs.9b03488>.
- (7) Abe, M. Diradicals. *Chem. Rev.* **2013**, *113* (9), 7011–7088. <https://doi.org/10.1021/cr400056a>.



- (8) Nakano, M.; Minami, T.; Yoneda, K.; Muhammad, S.; Kishi, R.; Shigeta, Y.; Kubo, T.; Rougier, L.; Champagne, B.; Kamada, K.; Ohta, K. Giant Enhancement of the Second Hyperpolarizabilities of Open-Shell Singlet Polyaromatic Diphenalenyl Diradicaloids by an External Electric Field and Donor–Acceptor Substitution. *J. Phys. Chem. Lett.* **2011**, *2* (9), 1094–1098. <https://doi.org/10.1021/jz200383a>.
- (9) Nakano, M.; Kishi, R.; Takebe, A.; Nate, M.; Takahashi, H.; Kubo, T.; Kamada, K.; Ohta, K.; Champagne, B.; Botek, E. Second Hyperpolarizability of Zethrenes. *Comput. Lett.* **2007**, *3*, 333–338. <https://doi.org/10.1163/157404007782913435>.
- (10) Nakano, M.; Kishi, R.; Nakagawa, N.; Ohta, S.; Takahashi, H.; Furukawa, S.; Kamada, K.; Ohta, K.; Champagne, B.; Botek, E.; Yamada, S.; Yamaguchi, K. Second Hyperpolarizabilities ( $\gamma$ ) of Bisimidazole and Bistriazole Benzenes: Diradical Character, Charged State, and Spin State Dependences. *J. Phys. Chem. A* **2006**, *110* (12), 4238–4243. <https://doi.org/10.1021/jp056672z>.
- (11) Nakano, M.; Kishi, R.; Nitta, T.; Kubo, T.; Nakasuji, K.; Kamada, K.; Ohta, K.; Champagne, B.; Botek, E.; Yamaguchi, K. Second Hyperpolarizability ( $\gamma$ ) of Singlet Diradical System: Dependence of  $\gamma$  on the Diradical Character. *J. Phys. Chem. A* **2005**, *109* (5), 885–891. <https://doi.org/10.1021/jp046322x>.
- (12) Nakano, M.; Kishi, R.; Ohta, S.; Takahashi, H.; Kubo, T.; Kamada, K.; Ohta, K.; Botek, E.; Champagne, B. Relationship between Third-Order Nonlinear Optical Properties and Magnetic Interactions in Open-Shell Systems: A New Paradigm for Nonlinear Optics. *Phys. Rev. Lett.* **2007**, *99* (3), 033001. <https://doi.org/10.1103/PhysRevLett.99.033001>.
- (13) Smith, M. B.; Michl, J. Singlet Fission. *Chem. Rev.* **2010**, *110* (11), 6891–6936. <https://doi.org/10.1021/cr1002613>.
- (14) Wen, J.; Havlas, Z.; Michl, J. Captodatively Stabilized Biradicaloids as Chromophores for Singlet Fission. *J. Am. Chem. Soc.* **2015**, *137* (1), 165–172. <https://doi.org/10.1021/ja5070476>.
- (15) Lukman, S.; Richter, J. M.; Yang, L.; Hu, P.; Wu, J.; Greenham, N. C.; Musser, A. J. Efficient Singlet Fission and Triplet-Pair Emission in a Family of Zethrene Diradicaloids. *J. Am. Chem. Soc.* **2017**, *139* (50), 18376–18385. <https://doi.org/10.1021/jacs.7b10762>.
- (16) Ullrich, T.; Pinter, P.; Messelberger, J.; Haines, P.; Kaur, R.; Hansmann, M. M.; Munz, D.; Guldi, D. M. Singlet Fission in Carbene-Derived Diradicaloids. *Angewandte Chemie International Edition* **2020**, *59* (20), 7906–7914. <https://doi.org/10.1002/anie.202001286>.
- (17) Ullrich, T.; Munz, D.; Guldi, D. M. Unconventional Singlet Fission Materials. *Chem. Soc. Rev.* **2021**, *50* (5), 3485–3518. <https://doi.org/10.1039/D0CS01433H>.
- (18) Minami, T.; Nakano, M. Diradical Character View of Singlet Fission. *J. Phys. Chem. Lett.* **2012**, *3* (2), 145–150. <https://doi.org/10.1021/jz2015346>.
- (19) Moore, J. H. Investigation of the Low Energy Singlet-Triplet and Singlet-Singlet Transitions in Ethylene Derivatives by Ion Impact. *J. Phys. Chem.* **1972**, *76* (8), 1130–1133. <https://doi.org/10.1021/j100652a007>.
- (20) Jones, R. R.; Bergman, R. G. P-Benzyne. Generation as an Intermediate in a Thermal Isomerization Reaction and Trapping Evidence for the 1,4-Benzenediyl Structure. *J. Am. Chem. Soc.* **1972**, *94* (2), 660–661. <https://doi.org/10.1021/ja00757a071>.
- (21) Bergman, R. G. Reactive 1,4-Dehydroaromatics. *Acc. Chem. Res.* **1973**, *6* (1), 25–31. <https://doi.org/10.1021/ar50061a004>.
- (22) Dressler, J. J.; Haley, M. M. Learning How to Fine-Tune Diradical Properties by Structure Refinement. *Journal of Physical Organic Chemistry* **2020**, *33* (11), e4114. <https://doi.org/10.1002/poc.4114>.
- (23) Rudebusch, G. E.; Zafra, J. L.; Jorner, K.; Fukuda, K.; Marshall, J. L.; Arrechea-Marcos, I.; Espejo, G. L.; Ponce Ortiz, R.; Gómez-García, C. J.; Zakharov, L. N.; Nakano, M.; Ottosson, H.; Casado, J.; Haley, M. M. Diindeno-Fusion of an Anthracene as a Design Strategy for Stable Organic Biradicals. *Nature Chem* **2016**, *8* (8), 753–759. <https://doi.org/10.1038/nchem.2518>.
- (24) Dressler, J. J.; Teraoka, M.; Espejo, G. L.; Kishi, R.; Takamuku, S.; Gómez-García, C. J.; Zakharov, L. N.; Nakano, M.; Casado, J.; Haley, M. M. Thiophene and Its Sulfur Inhibit Indenoindenodibenzothiophene Diradicals from Low-Energy Lying Thermal Triplets. *Nature Chem* **2018**, *10* (11), 1134–1140. <https://doi.org/10.1038/s41557-018-0133-5>.
- (25) Barker, J. E.; Dressler, J. J.; Cárdenas Valdivia, A.; Kishi, R.; Strand, E. T.; Zakharov, L. N.; MacMillan, S. N.; Gómez-García, C. J.; Nakano, M.; Casado, J.; Haley, M. M. Molecule Isomerism

- Modulates the Diradical Properties of Stable Singlet Diradicaloids. *J. Am. Chem. Soc.* **2020**, *142* (3), 1548–1555. <https://doi.org/10.1021/jacs.9b11898>.
- (26) Frederickson, C. K.; Rose, B. D.; Haley, M. M. Explorations of the Indenofluorenes and Expanded Quinoidal Analogues. *Acc. Chem. Res.* **2017**, *50* (4), 977–987. <https://doi.org/10.1021/acs.accounts.7b00004>.
- (27) Hayashi, H.; Barker, J. E.; Cárdenas Valdivia, A.; Kishi, R.; MacMillan, S. N.; Gómez-García, C. J.; Miyauchi, H.; Nakamura, Y.; Nakano, M.; Kato, S.; Haley, M. M.; Casado, J. Monoradicals and Diradicals of Dibenzofluoreno[3,2-b]Fluorene Isomers: Mechanisms of Electronic Delocalization. *J. Am. Chem. Soc.* **2020**, *142* (48), 20444–20455. <https://doi.org/10.1021/jacs.0c09588>.
- (28) Frederickson, C. K.; Zakharov, L. N.; Haley, M. M. Modulating Paratropicity Strength in Diareno-Fused Antiaromatics. *J. Am. Chem. Soc.* **2016**, *138* (51), 16827–16838. <https://doi.org/10.1021/jacs.6b11397>.
- (29) Clar, E. *Polycyclic Hydrocarbons*; London: Academic Press.
- (30) Clar, E. (1972). *The Aromatic Sextet*. New York, NY: Wiley.
- (31) Clar, E.; Zander, M. 378. 1: 12-2: 3-10: 11-Tribenzoperylene. *J. Chem. Soc.* **1958**, No. 0, 1861–1865. <https://doi.org/10.1039/JR9580001861>.
- (32) Zeng, Z.; Shi, X.; Chi, C.; Navarrete, J. T. L.; Casado, J.; Wu, J. Pro-Aromatic and Anti-Aromatic  $\pi$ -Conjugated Molecules: An Irresistible Wish to Be Diradicals. *Chem. Soc. Rev.* **2015**, *44* (18), 6578–6596. <https://doi.org/10.1039/C5CS00051C>.
- (33) Stuyver, T.; Chen, B.; Zeng, T.; Geerlings, P.; De Proft, F.; Hoffmann, R. Do Diradicals Behave Like Radicals? *Chem. Rev.* **2019**, *119* (21), 11291–11351. <https://doi.org/10.1021/acs.chemrev.9b00260>.
- (34) Konishi, A.; Hirao, Y.; Nakano, M.; Shimizu, A.; Botek, E.; Champagne, B.; Shiomi, D.; Sato, K.; Takui, T.; Matsumoto, K.; Kurata, H.; Kubo, T. Synthesis and Characterization of Teranthene: A Singlet Biradical Polycyclic Aromatic Hydrocarbon Having Kekulé Structures. *J. Am. Chem. Soc.* **2010**, *132* (32), 11021–11023. <https://doi.org/10.1021/ja1049737>.
- (35) Konishi, A.; Hirao, Y.; Matsumoto, K.; Kurata, H.; Kishi, R.; Shigeta, Y.; Nakano, M.; Tokunaga, K.; Kamada, K.; Kubo, T. Synthesis and Characterization of Quarteranthene: Elucidating the Characteristics of the Edge State of Graphene Nanoribbons at the Molecular Level. *J. Am. Chem. Soc.* **2013**, *135* (4), 1430–1437. <https://doi.org/10.1021/ja309599m>.
- (36) Ajayakumar, M. R.; Fu, Y.; Ma, J.; Hennesdorf, F.; Komber, H.; Weigand, J. J.; Alfonso, A.; Popov, A. A.; Berger, R.; Liu, J.; Müllen, K.; Feng, X. Toward Full Zigzag-Edged Nanographenes: Peri-Tetracene and Its Corresponding Circumanthracene. *J. Am. Chem. Soc.* **2018**, *140* (20), 6240–6244. <https://doi.org/10.1021/jacs.8b03711>.
- (37) Zöphel, L.; Berger, R.; Gao, P.; Enkelmann, V.; Baumgarten, M.; Wagner, M.; Müllen, K. Toward the Peri-Pentacene Framework. *Chemistry – A European Journal* **2013**, *19* (52), 17821–17826. <https://doi.org/10.1002/chem.201302859>.
- (38) Ajayakumar, M. R.; Ma, J.; Lucotti, A.; Schellhammer, K. S.; Serra, G.; Dmitrieva, E.; Rosenkranz, M.; Komber, H.; Liu, J.; Ortman, F.; Tommasini, M.; Feng, X. Persistent Peri-Heptacene: Synthesis and In Situ Characterization. *Angewandte Chemie International Edition* **2021**, *60* (25), 13853–13858. <https://doi.org/10.1002/anie.202102757>.
- (39) Ohashi, K.; Kubo, T.; Masui, T.; Yamamoto, K.; Nakasuji, K.; Takui, T.; Kai, Y.; Murata, I. 4,8,12,16-Tetra-Tert-Butyl-s-Indaceno[1,2,3-Cd:5,6,7-c'd']Diphenalene: A Four-Stage Amphoteric Redox System. *J. Am. Chem. Soc.* **1998**, *120* (9), 2018–2027. <https://doi.org/10.1021/ja970961m>.
- (40) Kubo, T.; Sakamoto, M.; Akabane, M.; Fujiwara, Y.; Yamamoto, K.; Akita, M.; Inoue, K.; Takui, T.; Nakasuji, K. Four-Stage Amphoteric Redox Properties and Biradicaloid Character of Tetra-Tert-Butyldicyclopenta[b;d]Thieno[1,2,3-Cd:5,6,7-C'd']Diphenalene. *Angewandte Chemie International Edition* **2004**, *43* (47), 6474–6479. <https://doi.org/10.1002/anie.200460565>.
- (41) Shimizu, A.; Kubo, T.; Uruichi, M.; Yakushi, K.; Nakano, M.; Shiomi, D.; Sato, K.; Takui, T.; Hirao, Y.; Matsumoto, K.; Kurata, H.; Morita, Y.; Nakasuji, K. Alternating Covalent Bonding Interactions in a One-Dimensional Chain of a Phenalenyl-Based Singlet Biradical Molecule Having Kekulé Structures. *J. Am. Chem. Soc.* **2010**, *132* (41), 14421–14428. <https://doi.org/10.1021/ja1037287>.
- (42) Sun, Z.; Huang, K.-W.; Wu, J. Soluble and Stable Heptazethrenebis(Dicarboximide) with a Singlet Open-Shell Ground State. *J. Am. Chem. Soc.* **2011**, *133* (31), 11896–11899. <https://doi.org/10.1021/ja204501m>.

- (43) Li, Y.; Heng, W.-K.; Lee, B. S.; Aratani, N.; Zafra, J. L.; Bao, N.; Lee, R.; Sung, Y. M.; Sun, Z.; Huang, K.-W.; Webster, R. D.; López Navarrete, J. T.; Kim, D.; Osuka, A.; Casado, J.; Ding, J.; Wu, J. Kinetically Blocked Stable Heptazethrene and Octazethrene: Closed-Shell or Open-Shell in the Ground State? *J. Am. Chem. Soc.* **2012**, *134* (36), 14913–14922. <https://doi.org/10.1021/ja304618v>.
- (44) Sun, Z.; Lee, S.; Park, K. H.; Zhu, X.; Zhang, W.; Zheng, B.; Hu, P.; Zeng, Z.; Das, S.; Li, Y.; Chi, C.; Li, R.-W.; Huang, K.-W.; Ding, J.; Kim, D.; Wu, J. Dibenzoheptazethrene Isomers with Different Biradical Characters: An Exercise of Clar's Aromatic Sextet Rule in Singlet Biradicaloids. *J. Am. Chem. Soc.* **2013**, *135* (48), 18229–18236. <https://doi.org/10.1021/ja410279j>.
- (45) Huang, R.; Phan, H.; Heng, T. S.; Hu, P.; Zeng, W.; Dong, S.; Das, S.; Shen, Y.; Ding, J.; Casanova, D.; Wu, J. Higher Order  $\pi$ -Conjugated Polycyclic Hydrocarbons with Open-Shell Singlet Ground State: Nonazethrene versus Nonacene. *J. Am. Chem. Soc.* **2016**, *138* (32), 10323–10330. <https://doi.org/10.1021/jacs.6b06188>.
- (46) Zeng, Z.; Sung, Y. M.; Bao, N.; Tan, D.; Lee, R.; Zafra, J. L.; Lee, B. S.; Ishida, M.; Ding, J.; López Navarrete, J. T.; Li, Y.; Zeng, W.; Kim, D.; Huang, K.-W.; Webster, R. D.; Casado, J.; Wu, J. Stable Tetrabenzo-Chichibabin's Hydrocarbons: Tunable Ground State and Unusual Transition between Their Closed-Shell and Open-Shell Resonance Forms. *J. Am. Chem. Soc.* **2012**, *134* (35), 14513–14525. <https://doi.org/10.1021/ja3050579>.
- (47) Zeng, W.; Qi, Q.; Wu, J. Toward Long Rylene Ribbons and Quinoidal Rylene Diradicaloids. *European Journal of Organic Chemistry* **2018**, *2018* (1), 7–17. <https://doi.org/10.1002/ejoc.201701352>.
- (48) Zeng, W.; Phan, H.; Heng, T. S.; Gopalakrishna, T. Y.; Aratani, N.; Zeng, Z.; Yamada, H.; Ding, J.; Wu, J. Rylene Ribbons with Unusual Diradical Character. *Chem* **2017**, *2* (1), 81–92. <https://doi.org/10.1016/j.chempr.2016.12.001>.
- (49) Doehnert, D.; Koutecky, J. Occupation Numbers of Natural Orbitals as a Criterion for Biradical Character. Different Kinds of Biradicals. *J. Am. Chem. Soc.* **1980**, *102* (6), 1789–1796. <https://doi.org/10.1021/ja00526a005>.
- (50) Yamaguchi, K.; Kawakami, T.; Takano, Y.; Kitagawa, Y.; Yamashita, Y.; Fujita, H. Analytical and Ab Initio Studies of Effective Exchange Interactions, Polyradical Character, Unpaired Electron Density, and Information Entropy in Radical Clusters (R)<sub>N</sub>: Allyl Radical Cluster (N=2–10) and Hydrogen Radical Cluster (N=50). *International Journal of Quantum Chemistry* **2002**, *90* (1), 370–385. <https://doi.org/10.1002/qua.979>.
- (51) Shen, J.-J.; Han, Y.; Dong, S.; Phan, H.; Heng, T. S.; Xu, T.; Ding, J.; Chi, C. A Stable [4,3]Peri-Acene Diradicaloid: Synthesis, Structure, and Electronic Properties. *Angewandte Chemie International Edition* **2021**, *60* (9), 4464–4469. <https://doi.org/10.1002/anie.202012328>.
- (52) Frontiers | Forty years of Clar's aromatic  $\pi$ -sextet rule | Chemistry <https://www.frontiersin.org/articles/10.3389/fchem.2013.00022/full> (accessed 2021 -11 -23).
- (53) Clar, E.; Stewart, D. G. Aromatic Hydrocarbons. LXV. Triangulene Derivatives1. *J. Am. Chem. Soc.* **1953**, *75* (11), 2667–2672. <https://doi.org/10.1021/ja01107a035>.
- (54) Clar, E.; Stewart, D. G. Aromatic Hydrocarbons. LXVIII. Triangulene Derivatives. Part II1. *J. Am. Chem. Soc.* **1954**, *76* (13), 3504–3507. <https://doi.org/10.1021/ja01642a044>.
- (55) Inoue, J.; Fukui, K.; Kubo, T.; Nakazawa, S.; Sato, K.; Shiomi, D.; Morita, Y.; Yamamoto, K.; Takui, T.; Nakasuji, K. The First Detection of a Clar's Hydrocarbon, 2,6,10-Tri-Tert-Butyltriangulene: A Ground-State Triplet of Non-Kekulé Polynuclear Benzenoid Hydrocarbon. *J. Am. Chem. Soc.* **2001**, *123* (50), 12702–12703. <https://doi.org/10.1021/ja016751y>.
- (56) Pavliček, N.; Mistry, A.; Majzik, Z.; Moll, N.; Meyer, G.; Fox, D. J.; Gross, L. Synthesis and Characterization of Triangulene. *Nature Nanotechnology* **2017**, *12* (4), 308–311. <https://doi.org/10.1038/nnano.2016.305>.
- (57) Arikawa, S.; Shimizu, A.; Shiomi, D.; Sato, K.; Shintani, R. Synthesis and Isolation of a Kinetically Stabilized Crystalline Triangulene. *J. Am. Chem. Soc.* **2021**. <https://doi.org/10.1021/jacs.1c10151>.
- (58) Li, Y.; Huang, K.-W.; Sun, Z.; Webster, R. D.; Zeng, Z.; Zeng, W.; Chi, C.; Furukawa, K.; Wu, J. A Kinetically Blocked 1,14:11,12-Dibenzopentacene: A Persistent Triplet Diradical of a Non-Kekulé Polycyclic Benzenoid Hydrocarbon. *Chem. Sci.* **2014**, *5* (5), 1908–1914. <https://doi.org/10.1039/C3SC53015A>.
- (59) Koga, Y.; Kaneda, T.; Saito, Y.; Murakami, K.; Itami, K. Synthesis of Partially and Fully Fused Polyaromatics by Annulative Chlorophenylene Dimerization. *Science* **2018**, *359* (6374), 435–439. <https://doi.org/10.1126/science.aap9801>.

- (60) Ito, H.; Ozaki, K.; Itami, K. Annulative  $\pi$ -Extension (APEX): Rapid Access to Fused Arenes, Heteroarenes, and Nanographenes. *Angewandte Chemie International Edition* **2017**, *56* (37), 11144–11164. <https://doi.org/10.1002/anie.201701058>.
- (61) Krzeszewski, M.; Ito, H.; Itami, K. Infinitene: A Helically Twisted Figure-Eight [12]Circulene Topoisomer. *J. Am. Chem. Soc.* **2021**. <https://doi.org/10.1021/jacs.1c10807>.
- (62) Scott, L. T.; Boorum, M. M.; McMahan, B. J.; Hagen, S.; Mack, J.; Blank, J.; Wegner, H.; de Meijere, A. A Rational Chemical Synthesis of C<sub>60</sub>. *Science* **2002**, *295* (5559), 1500–1503. <https://doi.org/10.1126/science.1068427>.
- (63) Scott, L. T. Methods for the Chemical Synthesis of Carbon Nanotubes: An Approach Based on Hemispherical Polyarene Templates. *Pure and Applied Chemistry* **2017**, *89* (6), 809–820. <https://doi.org/10.1515/pac-2016-1222>.
- (64) Scott, L. T.; Hashemi, M. M.; Meyer, D. T.; Warren, H. B. Corannulene. A Convenient New Synthesis. *J. Am. Chem. Soc.* **1991**, *113* (18), 7082–7084. <https://doi.org/10.1021/ja00018a082>.
- (65) Zhao, L.; Prendergast, M. B.; Kaiser, R. I.; Xu, B.; Ablikim, U.; Ahmed, M.; Sun, B.-J.; Chen, Y.-L.; Chang, A. H. H.; Mohamed, R. K.; Fischer, F. R. Synthesis of Polycyclic Aromatic Hydrocarbons by Phenyl Addition–Dehydrocyclization: The Third Way. *Angewandte Chemie International Edition* **2019**, *58* (48), 17442–17450. <https://doi.org/10.1002/anie.201909876>.
- (66) Blackwell, R. E.; Zhao, F.; Brooks, E.; Zhu, J.; Piskun, I.; Wang, S.; Delgado, A.; Lee, Y.-L.; Louie, S. G.; Fischer, F. R. Spin Splitting of Dopant Edge States in Magnetic Zigzag Graphene Nanoribbons. *28*.
- (67) Haley, M. M.; Tykwinski, R. R. *Carbon-Rich Compounds: From Molecules to Materials*; John Wiley & Sons, 2006.
- (68) Kilde, M. D.; Murray, A. H.; Andersen, C. L.; Storm, F. E.; Schmidt, K.; Kadziola, A.; Mikkelsen, K. V.; Hampel, F.; Hammerich, O.; Tykwinski, R. R.; Nielsen, M. B. Synthesis of Radiaannulene Oligomers to Model the Elusive Carbon Allotrope 6,6,12-Graphyne. *Nat Commun* **2019**, *10* (1), 3714. <https://doi.org/10.1038/s41467-019-11700-0>.
- (69) Tykwinski, R. R. Synthesis of Unsymmetrical Derivatives of Pentacene for Materials Applications. *Acc. Chem. Res.* **2019**, *52* (8), 2056–2069. <https://doi.org/10.1021/acs.accounts.9b00216>.
- (70) Chalifoux, W. A.; Tykwinski, R. R. Synthesis of Polyynes to Model the Sp-Carbon Allotrope Carbyne. *Nature Chem* **2010**, *2* (11), 967–971. <https://doi.org/10.1038/nchem.828>.
- (71) Yang, W.; Lucotti, A.; Tommasini, M.; Chalifoux, W. A. Bottom-Up Synthesis of Soluble and Narrow Graphene Nanoribbons Using Alkyne Benzannulations. *J. Am. Chem. Soc.* **2016**, *138* (29), 9137–9144. <https://doi.org/10.1021/jacs.6b03014>.
- (72) Senese, A. D.; Chalifoux, W. A. Nanographene and Graphene Nanoribbon Synthesis via Alkyne Benzannulations. *Molecules* **2019**, *24* (1), 118. <https://doi.org/10.3390/molecules24010118>.
- (73) Alabugin, I. V.; Gonzalez-Rodriguez, E. Alkyne Origami: Folding Oligoalkynes into Polyaromatics. *Acc. Chem. Res.* **2018**, *51* (5), 1206–1219. <https://doi.org/10.1021/acs.accounts.8b00026>.
- (74) Haley, M. M. Synthesis and properties of annulenic subunits of graphyne and graphdiyne nanoarchitectures. *Pure and Applied Chemistry* **2008**, *80* (3), 519–532. <https://doi.org/10.1351/pac200880030519>.
- (75) Barker, J. E.; Price, T. W.; Karas, L. J.; Kishi, R.; MacMillan, S. N.; Zakharov, L. N.; Gómez-García, C. J.; Wu, J. I.; Nakano, M.; Haley, M. M. A Tale of Two Isomers: Enhanced Antiaromaticity/Diradical Character versus Deleterious Ring-Opening of Benzofuran-Fused s-Indacenes and Dicyclopenta[b,g]Naphthalenes. *Angewandte Chemie International Edition* **2021**, *60* (41), 22385–22392. <https://doi.org/10.1002/anie.202107855>.
- (76) Baumgartner, T. Insights on the Design and Electron-Acceptor Properties of Conjugated Organophosphorus Materials. *Acc. Chem. Res.* **2014**, *47* (5), 1613–1622. <https://doi.org/10.1021/ar500084b>.
- (77) Lovell, T. C.; Garrison, Z. R.; Jasti, R. Synthesis, Characterization, and Computational Investigation of Bright Orange-Emitting Benzothiadiazole [10]Cycloparaphenylene. *Angewandte Chemie* **2020**, *132* (34), 14469–14473. <https://doi.org/10.1002/ange.202006350>.
- (78) Chen, Z.; Mercer, J. A. M.; Zhu, X.; Romaniuk, J. A. H.; Pfattner, R.; Cegelski, L.; Martinez, T. J.; Burns, N. Z.; Xia, Y. Mechanochemical Unzipping of Insulating Polyadderene to Semiconducting Polyacetylene. *Science* **2017**, *357* (6350), 475–479. <https://doi.org/10.1126/science.aan2797>.

- (79) Jin, Z.; Teo, Y. C.; Teat, S. J.; Xia, Y. Regioselective Synthesis of [3]Naphthylenes and Tuning of Their Antiaromaticity. *J. Am. Chem. Soc.* **2017**, *139* (44), 15933–15939. <https://doi.org/10.1021/jacs.7b09222>.
- (80) Bergman, H. M.; Kiel, G. R.; Handford, R. C.; Liu, Y.; Tilley, T. D. Scalable, Divergent Synthesis of a High Aspect Ratio Carbon Nanobelt. *J. Am. Chem. Soc.* **2021**, *143* (23), 8619–8624. <https://doi.org/10.1021/jacs.1c04037>.
- (81) Lungerich, D.; Papaianina, O.; Feofanov, M.; Liu, J.; Devarajulu, M.; Troyanov, S. I.; Maier, S.; Amsharov, K. Dehydrative  $\pi$ -Extension to Nanographenes with Zig-Zag Edges. *Nat Commun* **2018**, *9* (1), 4756. <https://doi.org/10.1038/s41467-018-07095-z>.
- (82) Che, S.; Li, C.; Wang, C.; Zaheer, W.; Ji, X.; Phillips, B.; Gurbandurdyev, G.; Glynn, J.; Guo, Z.-H.; Al-Hashimi, M.; Zhou, H.-C.; Banerjee, S.; Fang, L. Solution-Processable Porous Graphitic Carbon from Bottom-up Synthesis and Low-Temperature Graphitization. *Chemical Science* **2021**, *12* (24), 8438–8444. <https://doi.org/10.1039/D1SC01902C>.
- (83) Müller, M.; Kübel, C.; Müllen, K. Giant Polycyclic Aromatic Hydrocarbons. *Chemistry – A European Journal* **1998**, *4* (11), 2099–2109. [https://doi.org/10.1002/\(SICI\)1521-3765\(19981102\)4:11<2099::AID-CHEM2099>3.0.CO;2-T](https://doi.org/10.1002/(SICI)1521-3765(19981102)4:11<2099::AID-CHEM2099>3.0.CO;2-T).
- (84) Cai, J.; Ruffieux, P.; Jaafar, R.; Bieri, M.; Braun, T.; Blankenburg, S.; Muoth, M.; Seitsonen, A. P.; Saleh, M.; Feng, X.; Müllen, K.; Fasel, R. Atomically Precise Bottom-up Fabrication of Graphene Nanoribbons. *Nature* **2010**, *466* (7305), 470–473. <https://doi.org/10.1038/nature09211>.
- (85) Spisak, S. N.; Zhou, Z.; Liu, S.; Xu, Q.; Wei, Z.; Kato, K.; Segawa, Y.; Itami, K.; Rogachev, A. Yu.; Petrukhina, M. A. Stepwise Generation of Mono-, Di-, and Triply-Reduced Warped Nanographenes: Charge-Dependent Aromaticity, Surface Nonequivalence, Swing Distortion, and Metal Binding Sites. *Angewandte Chemie International Edition* **2021**, *60* (48), 25445–25453. <https://doi.org/10.1002/anie.202110748>.
- (86) Moreno, C.; Vilas-Varela, M.; Kretz, B.; Garcia-Lekue, A.; Costache, M. V.; Paradinas, M.; Panighel, M.; Ceballos, G.; Valenzuela, S. O.; Peña, D.; Mugarza, A. Bottom-up Synthesis of Multifunctional Nanoporous Graphene. *Science* **2018**, *360* (6385), 199–203. <https://doi.org/10.1126/science.aar2009>.
- (87) Tsvetkov, N. P.; Gonzalez-Rodriguez, E.; Hughes, A.; dos Passos Gomes, G.; White, F. D.; Kuriakose, F.; Alabugin, I. V. Radical Alkyne Peri-Annulation Reactions for the Synthesis of Functionalized Phenalenes, Benzanthrenes, and Olympicene. *Angewandte Chemie International Edition* **2018**, *57* (14), 3651–3655. <https://doi.org/10.1002/anie.201712783>.
- (88) Gonzalez-Rodriguez, E.; Abdo, M. A.; dos Passos Gomes, G.; Ayad, S.; White, F. D.; Tsvetkov, N. P.; Hanson, K.; Alabugin, I. V. Twofold  $\pi$ -Extension of Polyarenes via Double and Triple Radical Alkyne Peri-Annulations: Radical Cascades Converging on the Same Aromatic Core. *J. Am. Chem. Soc.* **2020**, *142* (18), 8352–8366. <https://doi.org/10.1021/jacs.0c01856>.
- (89) Hughes, A. M.; dos Passos Gomes, G.; Alabugin, I. V. Stereoelectronic Influence of a “Spectator” Propargylic Substituent Can Override Aromaticity Effects in Radical Peri-Cyclizations En Route to Expanded Polyaromatics. *J. Org. Chem.* **2019**, *84* (4), 1853–1862. <https://doi.org/10.1021/acs.joc.8b02779>.
- (90) Di Motta, S.; Negri, F.; Fazzi, D.; Castiglioni, C.; Canesi, E. V. Biradicaloid and Polyenic Character of Quinoidal Oligothiophenes Revealed by the Presence of a Low-Lying Double-Exciton State. *J. Phys. Chem. Lett.* **2010**, *1* (23), 3334–3339. <https://doi.org/10.1021/jz101400d>.
- (91) Peterson, P. W.; Mohamed, R. K.; Alabugin, I. V. How to Lose a Bond in Two Ways — The Diradical/Zwitterion Dichotomy in Cycloaromatization Reactions. *European Journal of Organic Chemistry* **2013**, *2013* (13), 2505–2527. <https://doi.org/10.1002/ejoc.201201656>.
- (92) Zeng, W.; Gopalakrishna, T. Y.; Phan, H.; Tanaka, T.; Herng, T. S.; Ding, J.; Osuka, A.; Wu, J. Superoctazethrene: An Open-Shell Graphene-like Molecule Possessing Large Diradical Character but Still with Reasonable Stability. *Journal of the American Chemical Society* **2018**. <https://doi.org/10.1021/jacs.8b09075>.
- (93) Binet, L.; Gourier, D. Bistable Magnetic Resonance of Conduction Electrons in Solids. *J. Phys. Chem.* **1996**, *100* (44), 17630–17639. <https://doi.org/10.1021/jp962094y>.
- (94) Schleyer, P. von R.; Maerker, C.; Dransfeld, A.; Jiao, H.; van Eikema Hommes, N. J. R. Nucleus-Independent Chemical Shifts: A Simple and Efficient Aromaticity Probe. *J. Am. Chem. Soc.* **1996**, *118* (26), 6317–6318. <https://doi.org/10.1021/ja960582d>.

- (95) Chen, Z.; Wannere, C. S.; Corminboeuf, C.; Puchta, R.; Schleyer, P. von R. Nucleus-Independent Chemical Shifts (NICS) as an Aromaticity Criterion. *Chem. Rev.* **2005**, *105* (10), 3842–3888. <https://doi.org/10.1021/cr030088+>.
- (96) Nakada, K.; Fujita, M.; Dresselhaus, G.; Dresselhaus, M. S. Edge State in Graphene Ribbons: Nanometer Size Effect and Edge Shape Dependence. *Phys. Rev. B* **1996**, *54* (24), 17954–17961. <https://doi.org/10.1103/PhysRevB.54.17954>.
- (97) Wakabayashi, K.; Fujita, M.; Ajiki, H.; Sigrist, M. Electronic and Magnetic Properties of Nanographite Ribbons. *Phys. Rev. B* **1999**, *59* (12), 8271–8282. <https://doi.org/10.1103/PhysRevB.59.8271>.
- (98) Yazyev, O. V. Emergence of Magnetism in Graphene Materials and Nanostructures. *Rep. Prog. Phys.* **2010**, *73* (5), 056501. <https://doi.org/10.1088/0034-4885/73/5/056501>.
- (99) Son, Y.-W.; Cohen, M. L.; Louie, S. G. Half-Metallic Graphene Nanoribbons. *Nature* **2006**, *444* (7117), 347–349. <https://doi.org/10.1038/nature05180>.
- (100) Kimouche, A.; Ervasti, M. M.; Drost, R.; Halonen, S.; Harju, A.; Joensuu, P. M.; Sainio, J.; Liljeroth, P. Ultra-Narrow Metallic Armchair Graphene Nanoribbons. *Nat Commun* **2015**, *6* (1), 10177. <https://doi.org/10.1038/ncomms10177>.